

Effect of gas-transfer velocity parameterization choice on air-sea CO₂ fluxes in the North Atlantic and the European Arctic

Iwona Wrobel¹ and Jacek Piskozub¹

¹ Institute of Oceanology, Polish Academy of Sciences, Sopot, Poland

Correspondence to: I. Wróbel (iwrobel@iopan.gda.pl)

Abstract

The oceanic sink of carbon dioxide (CO₂) is an important part of the global carbon budget. Understanding uncertainties in the calculation of this net flux into the ocean is crucial for climate research. One of the sources of the uncertainty within this calculation is the parameterization chosen for the CO₂ gas transfer velocity. We used a recently developed software toolbox, called the FluxEngine, to estimate the monthly air-sea CO₂ fluxes for the extratropical North Atlantic Ocean, the European Arctic, and globally using several published quadratic and cubic wind speed parameterizations of the gas transfer velocity. The aim of the study is to constrain the uncertainty caused by the choice of parameterization in the North Atlantic. This region is a large oceanic sink of CO₂, and it is also a region characterised by strong winds, especially in winter but with good in situ data coverage. We show that the uncertainty in the parameterization is smaller in the North Atlantic and the Arctic than globally. It is as little as 5% in the North Atlantic and 4% in the European Arctic, in comparison to 9% for the global ocean when restricted to parameterizations with quadratic wind dependence. This uncertainty becomes 46%, 44% and 65% respectively, when all parameterization are considered. We suggest that this smaller uncertainty (5% and 4%) is caused by a combination of higher than global average wind speeds in the North Atlantic ($> 7 \text{ ms}^{-1}$) and lack of any seasonal changes in the direction of the flux direction within most of the region. We also compare the impact of using two different *in situ* pCO₂ datasets (Takahashi et al. (2009) and SOCAT) for the flux calculation. The annual fluxes using the two data sets differ by 8% in the North Atlantic and 19% in the European Arctic. The seasonal fluxes in the Arctic computed from two datasets disagree with each other possibly due to insufficient spatial and temporal data coverage, especially in winter.

1. Introduction

The region of extratropical North Atlantic Ocean, including the European Arctic, is a region responsible for the formation of deep ocean waters (see Talley (2013) for a recent review). This process, part of the global overturning circulation, makes the area a large sink of atmospheric CO₂ (Takahashi et al., 2002; Takahashi et al., 2009; Landschützer et al., 2014; Le Quéré et al., 2015). Therefore, there is a widespread interest in tracking the changes in the North Atlantic net carbon dioxide fluxes, especially as models appear to predict a decrease in the sink volume later this century (Halloran et al., 2015).

The trend and variations in the North Atlantic CO₂ sinks has been intensively studied since observations have shown it appears to be decreasing (Lefèvre et al., 2004). This decrease on inter-annual time scales has been confirmed by further studies (Schuster and Watson, 2007) and this trend has continued in recent years North of 40° N (Landschützer et al., 2013). It is not certain how many of these changes are the result of long-term changes, decadal changes in atmospheric forcing—namely the North Atlantic Oscillation (Gonzalez-Davila et al., 2007; Thomas et al., 2008; Gruber 2009; Watson et al., 2009) or changes in meridional overturning circulations (Pérez et al., 2013).

Recent assessments of the Atlantic and the Arctic net sea-air CO₂ fluxes (Schuster et al., 2013) and the global ocean net carbon uptake (Wanninkhof et al., 2013) show that the cause is still unknown.

To study the rate of the ocean CO₂ sink and especially its long-term trend, one needs to first constrain the uncertainty in the flux calculation. The global interannual air-sea CO₂ fluxes variability can be vary about 60% due to different in $p\text{CO}_2$ and 35% by k (Courtney et al., 2016). Sources of uncertainty include sampling coverage, the method of data interpolation, fugacity of CO₂ ($f\text{CO}_2$), the method used for normalization of fugacity data to a reference year in a world of ever increasing atmospheric CO₂ the measurement uncertainty in all the parameters used to calculate the fluxes (including partial pressure in water and air, bulk and skin water temperatures, air temperatures, wind speed etc.) and some which are not usually included in the calculations but most probably influence the flux values (sea state parameters, air bubble void fraction, surfactant effects etc.) as well as the choice of gas transfer velocity k parameterization formula (Landschützer et al., 2014; Woolf et al., 2015a, 2015b). It has also been identified that the choice of the wind data product provides an additional source of uncertainty in gas transfer velocity, even by 10% - 40% and choice of wind speed parameterization may cause a difference in the results of k , even about 50% (Gregg et al., 2014; Couldrey et al., 2016). In this work we analyze solely the effect of choice between various published empirical wind driven gas transfer parameterizations. The North Atlantic is one of the regions of the world ocean best covered by CO₂ fugacity measurements (Watson et al., 2011), the Arctic seas coverage is much poorer, especially in winter (Schuster et al., 2013).

One of the factors influencing the value of the calculated net air-sea gas flux is the choice of the formula for the gas transfer velocity. Within the literature there are many different parameterizations to choose from and most depend on a cubic or quadratic wind speed relationship. The choice of the appropriate parameterization is not trivial as indicated by the name of an international meeting which focused on this topic (“ k conundrum” workshop, COST-735 Action organized meeting in Norwich, February 2008). The conclusions from this meeting have been incorporated into a recent review book chapter (Garbe et al., 2014). This paper concentrates on quantifying the uncertainty caused by the choice of the gas transfer velocity parameterization in the North Atlantic and the European Arctic. These regions were chosen as they are the areas for which many of the parameterization were originally derived. They are also regions with wind fields skewed towards higher winds (in comparison to the global average) enabling the effect of stronger winds on the net flux calculations to be investigated by using published gas transfer velocity formulas.

2. Methods

2.1 Datasets

We calculated net air-sea CO₂ fluxes using a set of software processing tools called the ‘FluxEngine’ (Shutler et al., 2016), which was created within European Space Agency funded OceanFlux Greenhouse Gases project (<http://www.oceanflux-ghg.org>). All gas flux calculations were performed using the FluxEngine software. The tools were developed to provide the community with a verified and consistent toolbox and to encourage the use of satellite Earth Observation (EO) data for studying air-sea fluxes. The toolbox source code can be downloaded or alternatively there is a version that can be run through a web interface. Within the online web interface, a suite of reanalysis data products, *in situ* and model data are available as input to the toolbox. The FluxEngine allows you to select several different air-sea flux parameterizations, as well as input data, producing monthly global gridded net air-sea fluxes products with 1° x 1° spatial resolution. The output consists of twelve NetCDF files (one file per month). One monthly composite file includes the mean (first order moment), median, standard deviation and the second, third and fourth order moments. There is also information (meta data) about origin of data inputs.

Users can choose from all of the data available on the web portal; an example of monthly EO input data includes: rain intensity, wind speed and direction, % of sea ice cover from monthly model data, ECMWF air pressure, whitecapping (Goddijn-Murphy et al., 2011), two options for monthly datasets of $p\text{CO}_2$, SST, salinity. The user then needs to choose the different components and structure of the net air-sea gas flux calculation and choose the transfer velocity parameterization. For the calculations, we used $p\text{CO}_2$ and salinity values from Takahashi et al. (2009) climatology which is based on more than 3 million measurements of surface water $p\text{CO}_2$ in open-ocean environments during non El Nino conditions. For some calculations we used, as an alternative, Surface Ocean CO_2 Atlas (SOCAT) version 1.5 and 2.0 (Sabine et al., 2013; Pfeil et al., 2013; Bakker et al., 2014) $p\text{CO}_2$ and associated SST data. SOCAT is a community driven dataset containing 6.3 and 10.1 million surface water CO_2 fugacity values for version 1.5 and 2.0, respectively, with a global coverage. The SOCAT databases have been re-analysed and then converted to climatologies using the methodology described in Goddijn-Murphy et al. (2015). All the climatologies were calculated for year 2010 with the FluxEngine toolset. The SSTskin (defined within Group for High Resolution SST (GHRSSST) as temperature of the surface measured by an infrared radiometer operating at the depth of $\sim 10\text{-}20\ \mu\text{m}$) values were taken from the Advance Along Track Scanning Radiometer (ESA/ARC/(A)ATSR) Global Monthly Sea Surface dataset (Merchant et al., 2012) in the case of both datasets, and have been preprocessed in the same way for use with the FluxEngine (Shutler et al., 2016).

We used Earth Observation (EO) wind speed and sea roughness (σ_0 – altimeter backscatter signal in Ku band from GlobWave L2P products) data obtained from the European Space Agency (ESA). The GlobWave satellite products give a “uniform” set of along track satellite wave data from all available Altimeters (spanning multiple space agencies) and from ESA Synthetic Aperture Radar (SAR) data and are publicly available at the Ifremer/CERSAT cloud (<http://globwave.ifremer.fr/products/data-access>). GlobWave Project is funded by ESA and subsidised by Centre National d’Etudes Spatial (CNES). The aim of the project was to constrain a uniform, harmonized, quality controlled, multi-sensor set of satellite wind-wave data for using by different communities despite of *in situ* data. Wave data are collected from six altimeter missions (Topex/POSEIDON, Jason-1/22, CryoSAT, GEOSAT and GEOSAT Follow On) and from ESA Synthetic Aperture Radar (SAR) missions, namely ERS-1/2 and ENVISAT. All data come in netCDF-3 format.

All analyses were performed using global data within the FluxEngine software. From the gridded product ($1^\circ \times 1^\circ$) we extracted the extratropical North Atlantic (north of 30°N), and its subset, the European Arctic (north of 64°N). For comparison, we also calculated fluxes in the Southern Ocean (south of 40°S). Hereafter we follow the convention of that sources of CO_2 (upward ocean-to-atmosphere gas fluxes) are positive and sinks (downward atmosphere-to-ocean gas fluxes) are negative. We give all results of net CO_2 fluxes in the SI unit of Pg (Pg is $10^{15}\ \text{g}$ which is numerically identical to Gt).

2.2. k parameterizations

The flux of CO_2 at the interface of air and the sea is controlled by wind speed, sea state, sea surface temperature (SST) and other factors. We estimate the net air-sea flux of CO_2 (F , $\text{mg C m}^{-2}\ \text{day}^{-1}$) as the product of gas transfer velocity (k , ms^{-1}) and the difference in CO_2 concentration (gm^{-3}) in the sea water and its interface with the air (Land et al., 2013). The concentration of CO_2 in sea water is the product of its solubility (α , $\text{gm}^{-3}\ \mu\text{atm}^{-1}$) and its fugacity ($f\text{CO}_2$, μatm). Solubility is in turn, a function of salinity and temperature. Hence F is defined as:

$$F = k (\alpha_W f\text{CO}_{2W} - \alpha_S f\text{CO}_{2A}) \quad (1)$$

where the subscripts denote values in water (W) and the air-sea interface (S) and in the air (A). We can exchange fugacity with the partial pressure (their values differ by <0.5 % over the temperature range considered) (McGillis et al., 2001). So equation (1) now becomes:

$$F = k (\alpha_W p\text{CO}_{2W} - \alpha_S p\text{CO}_{2A}) \quad (2)$$

One can also ignore the differences between the two solubilities, and just use the waterside solubility α_W . Equation (2) will then become:

$$F = k \alpha_W (p\text{CO}_{2W} - p\text{CO}_{2A}) \quad (3)$$

This formulation is often referred to as the ‘bulk parametrization’.

In this study we chose to analyze the air-sea gas fluxes using five different gas transfer parameterizations (k). All of them are wind speed parameterizations, but differ in the formula used:

$$k = \sqrt{(660.0 / \text{Sc}_{\text{skin}})} * (0.212 U_{10}^2 + 0.318 U_{10}) \quad (4)$$

(Nightingale et al., 2000),

$$k = \sqrt{(660.0 / \text{Sc}_{\text{skin}})} * 0.254 U_{10}^2 \quad (5)$$

(Ho et al., 2006),

$$k = \sqrt{(660.0 / \text{Sc}_{\text{skin}})} * 0.0283 U_{10}^3 \quad (6)$$

(Wanninkhof and McGillis, 1999),

$$k = \sqrt{(660.0 / \text{Sc}_{\text{skin}})} * 0.251 U_{10}^2 \quad (7)$$

(Wanninkhof, 2014),

$$k = \sqrt{(660.0 / \text{Sc}_{\text{skin}})} * (3.3 + 0.026 U_{10}^3) \quad (8)$$

(McGillis et al., 2001),

where Sc_{skin} stands for the Schmidt numbers at the skin surface, a function of SST ($[= (\text{kinematic viscosity of water})/(\text{diffusion coefficient of CO}_2 \text{ in water})]$), 660.0 is the Schmidt number corresponding to values of carbon dioxide at 20 °C in seawater, U_{10} is the wind speed 10 m above the sea surface.

In addition to the purely wind driven parameterizations, we have used the combined Goddijn-Murphy et al. (2012) and Fangohr and Woolf (2007) parametrization, which was developed as a test algorithm within of OceanFlux GHG Evolution project. This parameterization separates contributions from direct- and bubble-mediated gas transfer as suggested by Woolf (2005). Its purpose is to enable a separate evaluation of the effect of the two processes on air-sea gas fluxes and it is an algorithm that has yet to be calibrated. We used two versions of this parameterization: wind driven direct transfer (using the U_{10} wind fields) and radar backscatter driven direct transfer (using mean wave square slope) as described in Goddijn-Murphy et al. (2012).

3. Results

Using the FluxEngine software, we have produced global gridded monthly net CO₂ air-sea fluxes and from these we have extracted the values for the two study regions, the extratropical North Atlantic Ocean and separately for its subset - the European Arctic seas. Figure 1 shows maps of the

monthly mean air-sea CO₂ fluxes for the North Atlantic, calculated with Nightingale et al. (2000) (hereafter called N2000) k parameterization and the Takahashi et al. (2009) climatology for the whole year and for each season. The area, as a whole, is a sink of CO₂ (from blue to purple colored in the Fig. 1) but in some parts, close to North Atlantic Drift and East Greenland Current, is net source (from yellow to red colored in the Fig. 1). At the seasonal maps one can see more variability affects by physical process or biological activity. For example, the areas close to the North Atlantic Drift And East Greenland current are sinks of CO₂ in the summer (likely due to the growth of phytoplankton) while the southern most areas of the region become CO₂ sources in summer and autumn (which is likely to be due to the effect of sea-water temperature changes). Much of this variability is caused by changes of the surface water $p\text{CO}_2$ average values, shown in Figure 2 for the whole year and for each season (and variability in atmospheric CO₂ partial pressure, not shown). However, the flux is proportional to the product of $\Delta p\text{CO}_2$ and k . In most parameterizations k is a function of wind speed (eqs. 4-8). The mean wind speed U_{10} for the whole year and each season are shown in Figure 3. The wind speeds in the North Atlantic are higher than the mean value in the world ocean (7 m s^{-1} ; Courtney et al., 2016), with mean values higher than 10 m s^{-1} in many regions of the study area in all seasons except for the summer (with highest values in winter). This is important because the air-sea flux depends not only on average wind speed but also on its distribution (see also the Discussion). This effect is especially visible between formulas with different powers of U_{10} . Figure 4 shows the difference in the air-sea CO₂ fluxes calculated using two example parameterizations: one proportional to U_{10}^3 (eq. 6) and one to U_{10}^2 (eq. 7), namely Wanninkhof and McGillis (1999) (hereafter called WMcG1999) and Wanninkhof (2014) (hereafter called W2014). It can be seen that the “cubic” function results in higher absolute air-sea flux values when compared to the “quadratic” function in the regions of high winds, and lower absolute air-sea flux values in weaker winds.

Figure 5 shows the monthly values of air-sea CO₂ fluxes for the five parameterizations (eq. 4-8) for the North Atlantic and the European Arctic. The regions are sinks of CO₂ in every month, although August is close to neutral for the North Atlantic. The results using cubic parameterizations (eqs. 6 and 8) are higher in absolute values, respectively by up to 30% for WMcG1999 and 55% for McGillis (2001) (hereafter called McG2001), in comparison to the “quadratic” of N2000 (eq. 4). The other two “quadratic” parameterizations W2014 and Ho et al. (2006) (hereafter called H2006) (eqs. 5 and 7) resulted in fluxes within 5% of N2000. Annual net fluxes for the North Atlantic and the European Arctic and global (included for comparison) are shown in Table 1. In addition to the five parameterizations Figure 6 presents results for both of the OceanFlux GHG Evolution formulas (using wind and radar backscatter data). The mean and standard deviations of the parameterization ensemble are shown as grey vertical lines. The standard deviation in global fluxes is similar to previous estimates (Sweeney et al., 2007, Landschützer et al., 2014) but they cannot be directly compared due to different parameterization choices and methodologies. The results show that the annual North Atlantic net air-sea CO₂ sink, depending on the formula used, varies from -0.38 Pg C for N2000 to -0.56 Pg C for McG2001. In the case of global net air-sea CO₂ sink the values are, respectively, -1.30 Pg C and -2.15 Pg C. Table 1 as well as Figure 6 shows the same data “normalized” to the N2000 data (divided by value), this allows us to visualize the relative differences. In the case of the North Atlantic using the “quadratic” W2014 and H2006 parameterizations results in a net air-sea flux that is, respectively, 4% and 5% higher in absolute value than the equivalent N2000 result, while the “cubic” WMcG1999 and McG2001 results in values that are up to 28% and 44% than N2000 results. The respective values for the Arctic are 3% for W2014 and 4% for H2006, as well as 28% for WMcG1999 and 44% for McG2001. In the case of global net air-sea CO₂ fluxes the equivalent values are 8% (W2014) and 9% (H2006) higher than the N2000 result for the quadratic functions as well as 33% (WMcG1999) and 65% (McG2001) for cubic ones. The OceanFlux GHG parameterization results, for the backscatter and wind-driven versions, in net air-sea CO₂ fluxes that are 38% and 47% higher for North Atlantic than the N2000

result and in the global case the values were 44% and 52% higher, respectively. The spread of the Arctic values was lower than the Atlantic ones (see Table 1). On the other hand, the values for the Southern Ocean were slightly higher than for the North Atlantic but lower than the global ones, with the exception of the OceanFlux GHG parameterizations.

All the above results were obtained with the Takahashi et al. (2009) $p\text{CO}_2$ climatology and for comparison, we have also calculated the air-sea CO_2 fluxes using the re-analysed SOCAT version 1.5 and 2.0 data (Goddijn-Murphy et al., 2015). Figure 7 shows the results using the N2000 k parameterization for all three of the datasets (Takahashi et al. (2009) and both SOCAT). In the case of the North Atlantic Ocean study area, although the monthly values show large differences (using both SOCAT datasets results in a larger sink in summer and smaller in winter compare to Takahashi et al. (2009)), the annual values are similar: -0.38 Pg C for both Takahashi et al. (2009) and SOCAT v1.5 and -0.41 Pg C for SOCAT v2.0. In the case of the European Arctic the situation is very different, with Takahashi et al. (2009) and SOCAT dataset derived climatologies resulting in inverse seasonal variability but with annual net air-sea CO_2 fluxes results that are similar: -0.102 Pg C for Takahashi et al. (2009), -0.085 Pg C for SOCAT v1.5 and -0.088 Pg C for SOCAT v2.0.

4. Discussion

Our results show that using the three “quadratic” parameterizations (Nightingale et al., 2000; Ho et al., 2006 and Wanninkhof, 2014) results in air-sea flux values that are within 5% of each other in the case of the North Atlantic. This discrepancy is smaller than the 9% difference identified for the global case (Fig. 6). This result above confirms that at present, these different parameterizations are interchangeable for the North Atlantic as this range is within the experimental uncertainty (Nightingale, 2015). The three parameterizations were derived using different methods and data from different regions, namely passive tracers and dual-trace experiments in the North Sea in the case of Nightingale et al. (2000), dual tracers in the Southern Ocean in the case of Ho et al. (2006), and global ocean ^{14}C inventories in the case of Wanninkhof (2014). The differences between the quadratic and cubic parameterization are large, and instead of the quadratic functions that are supported by several lines of evidence (see Garbe et. al., 2014 for discussion), the cubic function are not completely refuted by the available observation. Therefore, it is important to notice that a choice of one of the available cubic functions may lead to net air-sea CO_2 fluxes that are considerably larger in absolute values, by up to 33% in the North Atlantic and more than 50% globally.

The above results imply smaller relative differences between the parameterizations in the North Atlantic than globally. This is interesting because the North Atlantic is the region of strong winds and over most of its area there are no seasonal changes in the air-sea flux direction (Fig. 1). For example in the South Atlantic, the annual mean wind speed is 8.5 m s^{-1} (Takahashi et al., 2009), and of the CO_2 sink (south of 45°) decreases significantly after 1990 with increasing wind speeds; this may cause higher CO_2 concentration (and higher $p\text{CO}_2$) in surface water due to enhanced vertical mixing of CO_2 -rich deep waters (Le Quèrè et al., 2007) and biological activity (seasonal changes in primary production). Takahashi et al. (2009) also indicate that the air-sea CO_2 fluxes difference in the Southern Ocean is strongly dependent on the choice of the gas transfer parameterizations and wind speed. Smaller difference in the North Atlantic, than globally, are more surprising, given that at least some of the older parameterizations (e.g. W2009 or WMcG1999) were developed using a smaller range of winds than can exist in the North Atlantic. There may be two reasons for this. First, when comparing quadratic and cubic parameterizations (Fig. 8), the cubic parameterization implies higher air-sea fluxes for high winds, whereas the quadratic ones lead to higher fluxes for weaker winds. This difference can be presented in arithmetic terms. Let us assume two functions of wind speed U , $F_1(U)$ quadratic and $F_2(U)$ cubic:

$$F_1(U) = a U^2, \quad (9)$$

$$F_2(U) = b U^3. \quad (10)$$

The difference between the two functions ΔF is equal to:

$$\Delta F = F_2 - F_1 = b U^3 - a U^2 = b U^2 (U - a b^{-1}) = b U^2 (U - U_x) \quad (11)$$

where $U_x = a b^{-1}$. The difference is positive for wind speeds greater than U_x and negative for winds less U_x . U_x is the value of wind speed for which the two functions intersect. In the case of equations (6) and (7), where $a = 0.251$ and $b = 0.0283$, they imply that $U_x = 8.87 \text{ m s}^{-1}$. In fact all of the functions presented in Fig. 8 produce very similar values for U_x , all of which are close to 9 m s^{-1} . This value is very close to average wind speed in the North Atlantic (Fig. 3). This is one of the reasons of the small relative difference in net air-sea fluxes. The spread of flux values for the Southern Ocean seems to support this conclusion, being larger than that in the North Atlantic. The Southern Ocean has on average stronger winds than the North Atlantic (including also the Arctic Seas) which seems to have the smallest spread of flux values for different parameterizations. The other reason of smaller relative differences between the parameterizations in the North Atlantic than globally, is the lack of seasonal variation in the sign of the air-sea flux. In the case of seasonal changes in the air-sea flux direction (caused by seasonal changes in water temperature or primary productivity), with winds stronger than U_x in some seasons and weaker in others (usually strong winds in winter and weak in summer), the air-sea fluxes partly cancel each other while the difference between cubic and quadratic parameterizations add to each other due to simultaneous changes in the sign of both fluxes itself and the $U - U_x$ term. This effect of seasonal variation has been suggested to us based on available observations (A. Watson, University of Exeter– personal communication) but we are unaware of any paper investigating it or even describing it explicitly.

In addition to the five parameterizations described above, we calculated the air-sea fluxes using the OceanFlux GHG Evolution combined formula (Goddijn-Murphy et al., 2016), which parameterises the contributions from direct and bubble-mediated gas transfer into separate components. The resulting air-sea fluxes are higher in absolute terms, than all of the quadratic functions considered in this study, and are closer in value to cubic parameterization. This may mean that the bubble mediated term of Fangohr and Woolf (2007) is overestimating the bubble component, implying the need for a dedicated calibration effort. This question will be the subject of further studies in the OceanFlux GHG Evolution project.

Using both Takahashi et al. (2009) climatology and SOCAT datasets (Fig. 7) results in similar annual net air-sea CO_2 fluxes in the North Atlantic, it should be noted that they show different seasonal variations. This may have been caused by slightly different time periods of the datasets (i.e. the SOCAT based dataset contains more recent data). One have to remember that at present most of data from Takahashi et al. (2009) are included in SOCAT, so the differences, in the European Arctic, may be due to the underlying sparse data coverage and possible interpolation artifacts (Goddijn-Murphy et al., 2015) as well as processing of the data through the FluxEngine. The results are improved in Courtney et al. (2016) where modeled and observation data were compared and has been show the same relationships in high-latitude zone. This discrepancy makes us treat the net air-sea CO_2 fluxes results from the Arctic with much less confidence than the values for the whole North Atlantic. It is impossible to declare within this study which dataset is more accurate as only new data can settle this. However, new data, not included in the SOCAT version we used, have been available to the recent analysis by Yasunaka et al. (2016). The observed in-water $p\text{CO}_2$ data (Fig. 3 in Yasunaka et al., 2016), especially since 2005, show clearly an annual cycle compatible with the SOCAT seasonal flux variability.

5. Conclusions

In this paper we have studied the effect of the choice of gas transfer velocity parameterization on the net CO₂ air-sea gas fluxes in the North Atlantic and the European Arctic using the recently developed FluxEngine software. The results show that the uncertainty caused by the choice of the k formula is smaller in the North Atlantic and in the Arctic than it is globally. The difference in the annual net air-sea CO₂ fluxes caused by the choice of the parameterization is within 5% in the North Atlantic and 4% in the European Arctic, comparing to 9% globally for the studied functions with quadratic wind dependence. It is up to 46% different for the North Atlantic, 36% for the Arctic and 65% globally when comparing cubic and quadratic functions. In both cases the uncertainty in the North Atlantic and the Arctic regions are smaller than the global case. We explain the smaller North Atlantic variability to be a combination of, firstly, higher than global average wind speeds in the North Atlantic, close to 9 m s⁻¹, which is the wind speed at which most k parameterization have similar values, and secondly the all-season CO₂ sink conditions in most North Atlantic areas. We repeated the analysis using Takahashi et al. (2009) and SOCAT p CO₂ derived climatology and find that although the seasonal variability in the North Atlantic is different the annual net air-sea CO₂ fluxes are within 8% in the North Atlantic and 19% in the European Arctic. The seasonal flux calculated from the two p CO₂ datasets in the Arctic have inverse seasonal variations, indicating possible under sampling (aliasing) of the p CO₂ in this polar region and therefore highlighting the need to collect more polar p CO₂ observations in all months and seasons.

Acknowledgements

The publication has been financed from the funds of the Leading National Research Centre (KNOW) received by the Centre for Polar Studies for the period 2014-2018; OceanFlux Greenhouse Gases Evolution, a project funded by the European Space Agency, ESRIN Contract No. 4000112091/14/I-LG; and GAME "Growing of Marine Arctic Ecosystem", funded by Narodowe Centrum Nauki grant DEC-2012/04/A/NZ8/00661. We would also like to thank Jamie Shutler for important advice on the FluxEngine and for correct the manuscript for English language. The authors are very grateful to those who have produced and made freely available the LDEO Flux Climatology base, FluxEngine software funded by European Space Agency, Surface Ocean CO₂ Atlas (SOCAT), GlobWave Project funded by European Space Agency, as well as Centre de Recherche et d'Exploitation Satellitaire (CERSAT) at Ifremer.

References

- Bakker, D. C. E., Pfeil, B., Smith, K., Hankin, S., Olsen, A., Alin, S. R., Cosca, C., Harasawa, S., Kozyr, A., Nojiri, Y., O'Brien, K. M., Schuster, U., Telszewski, M., Tilbrook, B., Wada, C., Akl, J., Barbero, L., Bates, N. R., Boutin, J., Bozec, Y., Cai, W.-J., Castle, R. D., Chavez, F. P., Chen, L., Chierici, M., Currie, K., De Baar, H. J. W., Evans, W., Feely, R. A., Fransson, A., Gao, Z., Hales, B., Hardman-Mountford, N. J., Hoppema, M., Huang, W.-J., Hunt, C. W., Huss, B., Ichikawa, T., Johannessen, T., Jones, E. M., Jones, S. D., Jutterstrom, S., Kitidis, V., Kortzinger, A., Landschützer, P., Lauvset, S. K., Lefèvre, N., Manke, A. B., Mathis, J. T., Merlivat, L., Metzl, N., Murata, A., Newberger, T., Omar, A. M., Ono, T., Park, G.-H., Paterson, K., Pierrot, D., Ríos, A. F., Sabine, C. L., Saito, S., Salisbury, J., Sarma, V. V. S. S., Schlitzer, R., Sieger, R., Skjelvan, I., Steinhoff, T., Sullivan, K. F., Sun, H., Sutton, A. J., Suzuki, T., Sweeney, C., Takahashi, T., Tjiputra, J., Tsurushima, N., van Heuven, S. M. A. C., Vandemark, D., Vlahos, P., Wallace, D. W.

- R., Wanninkhof, R., and Watson, A. J.: An update to the Surface Ocean CO₂ Atlas (SOCAT version 2), *Earth Syst. Sci. Data*, 6: 69-90, doi:10.5194/essd-6-69-2014, 2014.
- Couldrey, M. P., Oliver, K. I. C., Yool, A., Halloran, P. R., Achterberg, E. P.: On which timescale do gas transfer velocities control North Atlantic CO₂ flux variability?, *Global Biogeochem. Cycles*, 2014.
- Donlon, C. J., Martin, M., Stark, J., Roberts-Jones, J., Fiedler, E., and Wimmer, W.: The Operational Sea Surface Temperature and Sea Ice Analysis (OSTIA) system, *Remote Sens. Environ.*, 116, 140-158, doi: 10.1016/j.rse.2010.10.017, 2011.
- Fangohr, S. and Woolf, D. K.: Application of new parameterizations of gas transfer velocity and their impact on regional and global marine CO₂ budgets, *J. Marine Syst.*, 66, 195-203, doi:10.1016/j.jmarsys.2006.01.012, 2007.
- Garbe, C. S., Rutgersson, A., Boutin, J., de Leeuw, G., Delille, B., Fairall, C. W., Gruber, N., Hare, J., Ho, D. T., Johnson, M. T., Nightingale, P. D., Pettersson, H., Piskozub, J., Sahlée, E., Tsai, W., Ward, B., Woolf, D. K., and Zappa, C. J.: Transfer across the air-sea Interface, in: *Ocean-atmosphere interactions of gases and particles*, edited by: Liss, P. S. and Johnson, M. T., *Earth Sys. Sci.*, Springer, Berlin, Heidelberg, 55–111, 2014.
- Goddijn-Murphy, L., Woolf, D. K., Callaghan, A. H.: Parameterizations and algorithms for oceanic whitecap coverage, *J. Phys. Oceanogr.*, 41, 742-756, doi:10.1175/2010JPO4533.1, 2011.
- Goddijn-Murphy, L. M., Woolf, D. K., and Marandino, C.: Space-based retrievals of air-sea gas transfer velocities using altimeters: Calibration for dimethyl sulfide, *J. Geophys. Res.*, 117, C08028, doi: 10.1029/2011JC007535, 2012.
- Goddijn-Murphy, L. M., Woolf, D. K., Land, P. E., Shutler J. D., Donlon, C.: The OceanFlux Greenhouse Gases methodology for deriving a sea surface climatology of CO₂ fugacity in support of air-sea gas flux studies, *Ocean Sci.*, 11, 519-541, doi: 10.5194/os-11-519-2015, 2015.
- Goddijn-Murphy, L., Woolf, D. K., Callaghan, A. H., Nightingale, P. D., and Shutler, J. D.: A reconciliation of empirical and mechanistic models of the air-sea gas transfer velocity, *J. Geophys. Res. Oceans*, 121, 818-835, doi:10.1002/2015JC011096, 2016.
- González-Dávila, M., Santana-Casiano, J. M., and González-Dávila, E. F.: Interannual variability of the upper ocean carbon cycle in the northeast Atlantic Ocean, *Geophys. Res. Lett.*, 34, L07608, doi: 10.1029/2006GL028145, 2007.
- Gregg, W. W., Casey, N. W., Rosseaux, C. S.: Sensitivity of simulated global ocean carbon flux estimates to forcing by reanalysis products, *Ocean Model.*, 80, 24-35, doi: 10.1016/j.ocemod.2014.05.002, 2014.
- Gruber, N.: Carbon cycle: Fickle trends in the ocean, *Nature*, 458, 155-156, doi: 10.1038/458155a, 2009.
- Halloran, P. R., Booth, B. B. B., Jones, C. D., Lambert, F. H., McNeall, D. J., Totterdell, I. J., and Völker, C.: The mechanisms of North Atlantic CO₂ uptake in a large Earth System Model ensemble, *Biogeosciences*, 12, 4497–4508, doi: 10.5194/bg-12-4497-2015, 2015.
- Ho, D. T., Law, C. S., Smith, M. J., Schlosser, P., Harvey, M., and Hill, P.: Measurements of air-sea

- gas exchange at high wind speeds in the Southern Ocean: Implications for global parameterizations, *Geophys. Res. Lett.*, 33, 16611, doi: 10.1029/2006/GL026817, 2006.
- Landschützer, P., Gruber, N., Bakker, D. C. E., Schuster, U., Nakaoka, S., Payne, M. R., Sasse, T. P., and Zeng, J.: A neural network-based estimate of the seasonal to inter-annual variability of the Atlantic Ocean carbon sink, *Biogeosciences*, 10, 7793-7815, doi: 10.5194/bg-10-7793-2013, 2013.
- Landschützer, P., Gruber, N., Bakker, D. C. E., Schuster, U.: Recent variability of the global ocean carbon sink, *Global Biogeochem. Cycles*, 28, 927–949, doi: 10.1002/2014GB004853, 2014.
- Le Quéré, C., Rödenbeck, C., Buitenhuis, E. T., Conway, T. J., Langenfelds, R., Gomez, A., Labuschagne, C., Ramonet, M., Nakazawa, T., Metzl, N., Gillett, N., Heimann, M.: Saturation of the Southern Ocean CO₂ sink due to recent climate change, *Science* 316, 1735-1738, doi:10.1126/science.1136188, 2007.
- Le Quéré, C., Moriarty, R., Andrew, R. M., Peters, G. P., Ciais, P., Friedlingstein, P., Jones, S. D., Sitch, S., Tans, P., Arneeth, A., Boden, T. A., Bopp, L., Bozec, Y., Canadell, J. G., Chini, L. P., Chevallier, F., Cosca, C. E., Harris, I., Hoppema, M., Houghton, R. A., House, J. I., Jain, A. K., Johannessen, T., Kato, E., Keeling, R. F., Kitidis, V., Klein Goldewijk, K., Koven, C., Landa, C. S., Landschützer, P., Lenton, A., Lima, I. D., Marland, G., Mathis, J. T., Metzl, N., Nojiri, Y., Olsen, A., Ono, T., Peng, S., Peters, W., Pfeil, B., Poulter, B., Raupach, M. R., Regnier, P., Rödenbeck, C., Saito, S., Salisbury, J. E., Schuster, U., Schwinger, J., Séférian, R., Segschneider, J., Steinhoff, T., Stocker, B. D., Sutton, A. J., Takahashi, T., Tilbrook, B., van der Werf, G. R., Viovy, N., Wang, Y.-P., Wanninkhof, R., Wiltshire, A., and Zeng, N.: Global carbon budget 2014, *Earth Syst. Sci. Data*, 7, 47–85, doi: 10.5194/essd-7-47-2015, 2015.
- Lefèvre, N., Watson, A. J., Olsen, A., Rios, A. F., Perez, F. F., Johannessen, T.: A decrease in the sink for atmospheric CO₂ in the North Atlantic, *Geophys. Res. Lett.*, 31, L07306, doi: 10.1029/2003GL018957, 2004.
- McGillis, W. R., and Edson, J. B., Hare, J. E., Fairall, C. W.: Direct covariance air-sea CO₂ fluxes, *J. Geophys. Res.*, 106, C8 16729-16745, 2001.
- Merchant, C. M., Embury, O., Rayner, N. A., Berry, D. I., Corlett, G. K., Lean, K., Veal, K. L., Kent, E. C., Llewellyn-Jones, D. T., Remedios, J. J., and Saunders, R.: A 20 year independent record of sea surface temperature for climate from Along-Track Scanning Radiometers, *J. Geophys. Res.*, 117, C12, doi:10.1029/2012JC008400, 2012.
- Nightingale, P. D., Malin, G., Law, C. S., Watson, A. J., Liss, P. S., Liddicoat, M. I., Boutin, J., and Upstill-Goddard, R. C.: In situ evaluation of air-sea gas exchange parameterizations using novel conservative and volatile tracers, *Global Biogeochem. Cycles*, 14, 373-387, 2000.
- Nightingale, P. D., Relationship between wind speed and gas exchange over the ocean: which parameterisation should I use? Report from Discussion Session at SOLAS Open Science conference in Kiel, <http://goo.gl/TrMQkg>, 2015.
- Orr, J. C., Maier-Reimer, E., Mikolajewicz, U., Monfray, P., Sarmiento, J. L., Toggweiler, J. R., Taylor, N. K., Palmer, J., Gruber, N., Sabine, C. L., Le Quéré, C., Key, R. M., Boutin, J.: Estimates of anthropogenic carbon uptake from four three-dimensional global ocean models, *Global Biogeochem. Cycles*, 15, 43-60, doi: 10.1029/2000GB001273, 2001.

511
512
513
514
515
516
517
518
519
520
521
522
523
524
525
526
527
528
529
530
531
532
533
534
535
536
537
538
539
540
541
542
543
544
545
546
547
548
549
550
551
552
553
554
555
556
557
558
559
560
561

Pérez, F. F., Mercier, H., Vázquez-Rodríguez, M., Lherminier, P., Velo, A., Pardo, P. C., Rosón, G., and Ríos, A. F.: Atlantic Ocean CO₂ uptake reduced by weakening of the meridional overturning circulation, *Nat. Geosci.*, 6, 146-152, doi: 10.1038/NGEO1680, 2013.

Pfeil, B., Olsen, A., Bakker, D. C. E., Hankin, S., Koyuk, H., Kozyr, A., Malczyk, J., Manke, A., Metzl, N., Sabine, C. L., Akl, J., Alin, S. R., Bates, N., Bellerby, R. G. J., Borges, A., Boutin, J., Brown, P. J., Cai, W.-J., Chavez, F. P., Chen, A., Cosca, C., Fassbender, A. J., Feely, R. A., González-Dávila, M., Goyet, C., Hales, B., Hardman-Mountford, N., Heinze, C., Hood, M., Hoppema, M., Hunt, C. W., Hydes, D., Ishii, M., Johannessen, T., Jones, S. D., Key, R. M., Körtzinger, A., Landschützer, P., Lauvset, S. K., Lefèvre, N., Lenton, A., Lourantou, A., Merlivat, L., Midorikawa, T., Mintrop, L., Miyazaki, C., Murata, A., Nakadate, A., Nakano, Y., Nakaoka, S., Nojiri, Y., Omar, A. M., Padin, X. A., Park, G.-H., Paterson, K., Perez, F. F., Pierrot, D., Poisson, A., Ríos, A. F., Santana-Casiano, J. M., Salisbury, J., Sarma, V. V. S. S., Schlitzer, R., Schneider, B., Schuster, U., Sieger, R., Skjelvan, I., Steinhoff, T., Suzuki, T., Takahashi, T., Tedesco, K., Telszewski, M., Thomas, H., Tilbrook, B., Tjiputra, J., Vandemark, D., Veness, T., Wanninkhof, R., Watson, A. J., Weiss, R., Wong, C. S., and Yoshikawa-Inoue, H.: A uniform, quality controlled Surface Ocean CO₂ Atlas (SOCAT), *Earth Syst. Sci. Data*, 5, 125-143, doi: 10.5194/essd-5-125-2013, 2013.

Sabine, C. L., Hankin, S., Koyuk, H., Bakker, D. C. E., Pfeil, B., Olsen, A., Metzl, N., Kozyr, A., Fassbender, A., Manke, A., Malczyk, J., Akl, J., Alin, S. R., Bellerby, R. G. J., Borges, A., Boutin, J., Brown, P. J., Cai, W.-J., Chavez, F. P., Chen, A., Cosca, C., Feely, R. A., González-Dávila, M., Goyet, C., Hardman-Mountford, N., Heinze, C., Hoppema, M., Hunt, C. W., Hydes, D., Ishii, M., Johannessen, T., Key, R. M., Körtzinger, A., Landschützer, P., Lauvset, S. K., Lefèvre, N., Lenton, A., Lourantou, A., Merlivat, L., Midorikawa, T., Mintrop, L., Miyazaki, C., Murata, A., Nakadate, A., Nakano, Y., Nakaoka, S., Nojiri, Y., Omar, A. M., Padin, X. A., Park, G.-H., Paterson, K., Perez, F. F., Pierrot, D., Poisson, A., Ríos, A. F., Salisbury, J., Santana-Casiano, J. M., Sarma, V. V. S. S., Schlitzer, R., Schneider, B., Schuster, U., Sieger, R., Skjelvan, I., Steinhoff, T., Suzuki, T., Takahashi, T., Tedesco, K., Telszewski, M., Thomas, H., Tilbrook, B., Vandemark, D., Veness, T., Watson, A. J., Weiss, R., Wong, C. S., and Yoshikawa-Inoue, H.: Surface Ocean CO₂ Atlas (SOCAT) gridded data products, *Earth Syst. Sci. Data*, 5, 145-153, doi: 10.5194/essd-5-145-2013, 2013.

Schuster, U., and Watson, A. J.: A variable and decreasing sink for atmospheric CO₂ in the North Atlantic, *J. Geophys. Res.*, 112, C11006, doi: 10.1029/2006JC003941, 2007.

Schuster, U., McKinley, G. A., Bates, N., Chevallier, F., Doney, S. C., Fay, A. R., González-Dávila, M., Gruber, N., Jones, S., Krijnen, J., Landschützer, P., Lefèvre, N., Manizza, M., Mathis, J., Metzl, N., Olsen, A., Rios, A. F., Rödenbeck, C., Santana-Casiano, J. M., Takahashi, T., Wanninkhof, R., and Watson, A. J.: An assessment of the Atlantic and Arctic sea-air CO₂ fluxes, 1990–2009, *Biogeosciences*, 10, 607–627, doi: 10.5194/bg-10-607-2013, 2013.

Shutler, J. D., Piolle, J-F., Land, P. E., Woolf, D. K., Goddijn-Murphy, L., Paul, F., Girard-Ardhuin, F., Chapron, B., and Donlon, C. J.: FluxEngine: a flexible processing system for calculating air-sea carbon dioxide gas fluxes and climatologies, *J. Atmos. Ocean. Tech.*, doi:10.1175/JTECH-D-14-00204.1, 2016.

Sweeney, C., Gloor, E., Jacobson, A. R., Key, R. M., McKinley, G., Sarmiento, J. L. and Wanninkhof, R.: Constraining global air-sea gas exchange for CO₂ with recent bomb 14C measurements, *Global Biogeochem. Cycles*, 21, doi:10.1029/2006GB002784, 2007.

- Takahashi, T., Sutherland, S. C., Sweeney, C., Poisson, A., Metzl, N., Tilbrook, B., Bates, N., Wanninkhof, R., Feely, R. A., Sabine, C., Olafsson, J., and Nojiri, Y.: Global sea-air CO₂ flux based on climatological surface ocean *p*CO₂, and seasonal biological and temperature effects, *Deep-Sea Res.*, Pt. II, 49, 1601-1622, 2002.
- Takahashi, T., Sutherland, S. C., Wanninkhof, R., Sweeney, C., Feely, R. A., Chipman, D. W., Hales, B., Friederich, G., Chavez, F., Sabine, C., Watson, A., Bakker, D. C. E., Schuster, U., Metzl, N., Yoshikawa-Inoue, H., Ishii, M., Midorikawa, T., Nojiri, Y., Körtzinger, A., Steinhoff, T., Hoppema, M., Olafsson, J., Arnarson, T. S., Tilbrook, B., Johannessen, T., Olsen, A., Bellerby, R., Wong, C. S., Delille, B., Bates, N. R., and de Baar, H. J. W.: Climatological mean and decadal change in surface ocean *p*CO₂ and net sea-air CO₂ flux over the global oceans, *Deep-Sea Res.* Pt. II, 56, 554–577, doi: 10.1016/j.dsr2.2008.12.009, 2009.
- Talley, L. D.: Closure of the global overturning circulation through the Indian, Pacific, and Southern Oceans: schematics and transports, *Oceanography* 26(1), 80–97, doi:10.5670/oceanog.2013.07, 2013.
- Thomas, H., Friederike Prowe, A. E., Lima, I. D., Doney, S. C., Wanninkhof, R., Greatbatch, R. J., Schuster, U., and Corbière, A.: Changes in the North Atlantic Oscillation influence CO₂ uptake in the North Atlantic over the past 2 decades, *Global Biogeochem. Cycles*, 22, GB4027, doi:10.1029/2007GB003167, 2008.
- Wanninkhof, R.: Relationship between wind speed and gas exchange over the ocean revisited, *Limnol. Oceanogr. Methods*, 12, 351–362, doi: 10.4319/lom.2014.12.351, 2014.
- Wanninkhof, R., and McGillis, W. R.: A cubic relationship between air-sea CO₂ exchange and wind speed, *Geophys. Res. Lett.*, 26, 1889-1892, 1999.
- Wanninkhof, R., Park, G.-H., Takahashi, T., Sweeney, C., Feely, R., Nojiri, Y., Gruber, N., Doney, S. C., McKinley, G. A., Lenton, A., Le Quéré, C., Heinze, C., Schwinger, J., Graven, H., Khatiwala, S.: Global ocean carbon uptake: magnitude, variability and trends, *Biogeosciences*, 10, 1983-2000, doi: 10.5194/bg-10-1983-2013, 2013.
- Watson, A. J., Schuster, U., Bakker, D. C. E., Bates, N. R., Corbière, A., González-Dávila, M., Friedrich, T., Hauck, J., Heinze, C., Johannessen, T., Körtzinger, A., Metzl, N., Olafsson, J., Olsen, A., Oschlies, A., Padin, X. A., Pfeil, B., Santana-Casiano, J. M., Steinhoff, T., Telszewski, M., Rios, A. F., Wallace, D. W., Wanninkhof, R.: Tracking the variable North Atlantic sink for atmospheric CO₂, *Science*, 326(5958), 1391-1393, doi: 10.1126/science.1177394, 2009.
- Watson, A. J., Metzl, N., Schuster, U.: Monitoring and interpreting the ocean uptake of atmospheric CO₂, *Philos. T. R. Soc. A*, 369, 1997–2008, doi: 10.1098/rsta.2011.0060, 2011.
- Woolf, D. K.: Parameterization of gas transfer velocities and sea-state dependent wave breaking. *Tellus B*, 57, 87–94, 2005.
- Woolf, D. K., Shutler, J. D., Goddijn-Murphy, L., Donlon, C. J., Nightingale, P. D., Land, P. E., Torres, R., Chapron, B., Piolle, J.-F., Herledan, S., Hanafin, J., Girard-Ardhuin, F., Ardhuin, F., Prytherch, J., Moat, B., and Yelland, M.: Key uncertainties in the contemporary air-sea flux of carbon dioxide: an OceanFlux study, submitted 2015a.

613 Woolf, D. K., Goddijn-Murphy, L. M., Shutler, J. D., Land, P. E., Donlon, C. J., Prytherch, J.,
 614 Yelland, M. J., Nightingale, P. D., Torres, R., Chapron, B., Piolle, J-F., Herledan, S., Hanafin, J.,
 615 Girard-Ardhuin, F., Ardhuin F., and Moat, B.: Sources and types of uncertainty in the
 616 contemporary air-sea flux of carbon dioxide: an OceanFlux study, submitted 2015b.
 617
 618 Yasunaka, S., Murata, A., Watanabe, E., Chierici, M., Fransson, A., van Heuven, S., Hoppema, M.,
 619 Ishii, M., Johannessen, T., Kosugi, N., Lauvset, S. K., Mathis, J. T., Nishino, S., Omar, A. M.,
 620 Olsen, A., Sasano, D., Takahashi, T., Wanninkhof, R.: Mapping of the air–sea CO₂ flux in the
 621 Arctic Ocean and its adjacent seas: Basin-wide distribution and seasonal to interannual
 622 variability, *Polar Sci.*, 1-12, doi:10.1016/j.polar.2016.03.006, 2016.

623 Figure 1. Seasonal and annual mean air-sea fluxes of CO₂ (mg C m⁻² day⁻¹) in the North Atlantic,
624 using Nightingale et al. (2000) *k* parameterization and Takahashi et al. (2009) climatology a)
625 annual, b) DJF (winter), c) MAM (spring), d) JJA (summer), e) SON (autumn). The gaps (white
626 areas) are due to missing data, land and ice masks.
627

628 Figure 2. Seasonal and annual *p*CO₂ values (µatm) in surface waters of the North Atlantic,
629 estimated using the Takahashi et al. (2009) climatology a) annual, b) DJF (winter), c) MAM
630 (spring), d) JJA (summer), e) SON (autumn). The gaps (white areas) are due to missing data, land
631 and ice masks.
632

633 Figure 3. Wind speed distribution *U*₁₀ (ms⁻¹) in the North Atlantic used to determine the relationship
634 between gas transfer velocity and air-sea CO₂ fluxes a) annual, b) DJF (winter), c) MAM (spring),
635 d) JJA (summer), e) SON (autumn). The gaps (white areas) are due to missing data, land and ice
636 masks.
637

638 Figure 4. Differences maps for the air-sea CO₂ fluxes (mg C m⁻² day⁻¹) in the North Atlantic,
639 between a cubed and a squared parameterization (Wanninkhof and McGillis 1999 and Wanninkhof
640 2014) a) annual, b) DJF (winter), c) MAM (spring), d) JJA (summer) e) SON (autumn). The gaps
641 (white areas) are due to missing data, land and ice masks.
642

643 Figure 5. Monthly values of CO₂ air-sea fluxes (Pg month⁻¹) for the five parameterizations (eq. 4-8)
644 a) the North Atlantic, b) the European Arctic.
645

646 Figure 6. Annual air-sea fluxes of CO₂ for the five (eq. 4-8) parameterizations as well as for
647 backscatter (default) and wind driven OceanFlux GHG parameterizations normalized to flux values
648 of Nightingale et al. (2000) *k* parameterization (see text) a) globally, b) the North Atlantic c) the
649 European Arctic, d) the Southern Ocean. Average values for all parameterization and standard
650 deviations are marked as vertical gray lines.
651

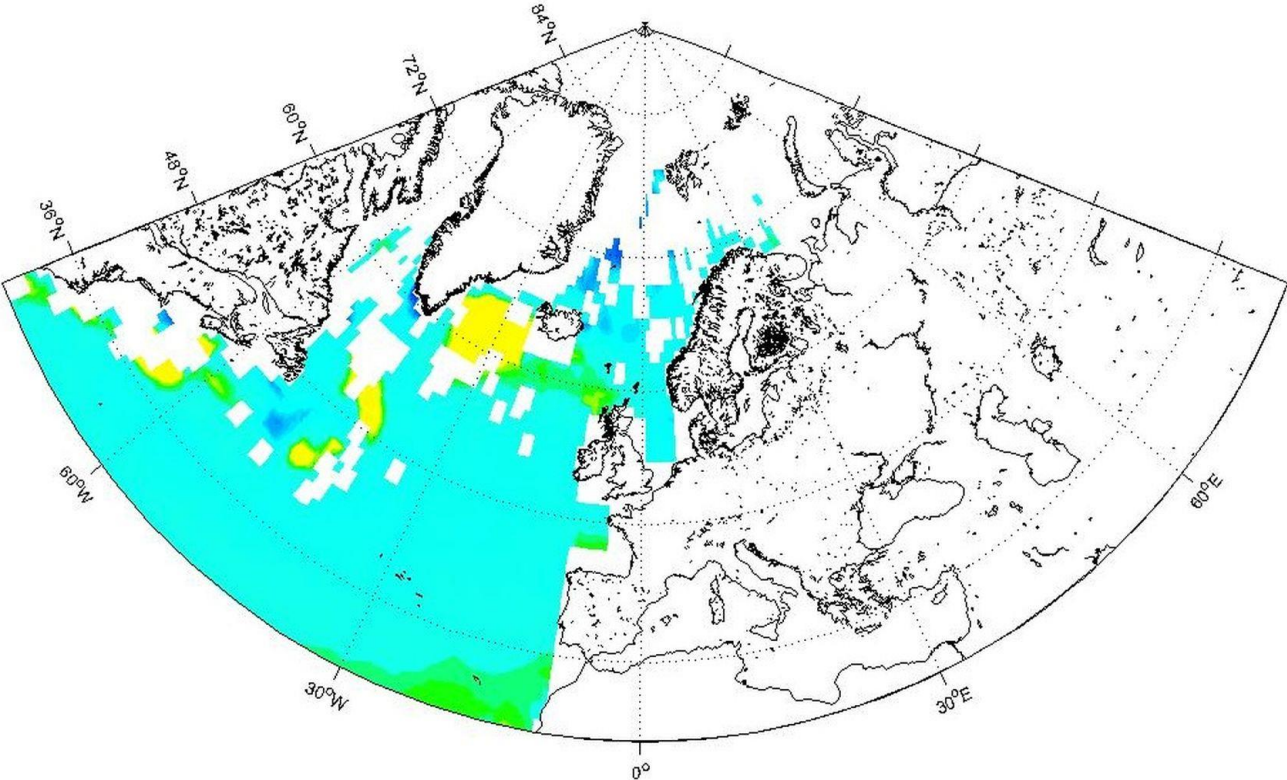
652 Figure 7. Comparison of monthly air-sea CO₂ fluxes calculated with different *p*CO₂ datasets
653 (Takahashi et al., 2009, SOCAT v. 1.5 and 2.0) using the same *k* parameterization (Nightingale et
654 al., 2000) a) the North Atlantic, b) the European Arctic.
655

656 Figure 8. Different *k*₆₆₀ parameterizations as a function of wind speed.
657

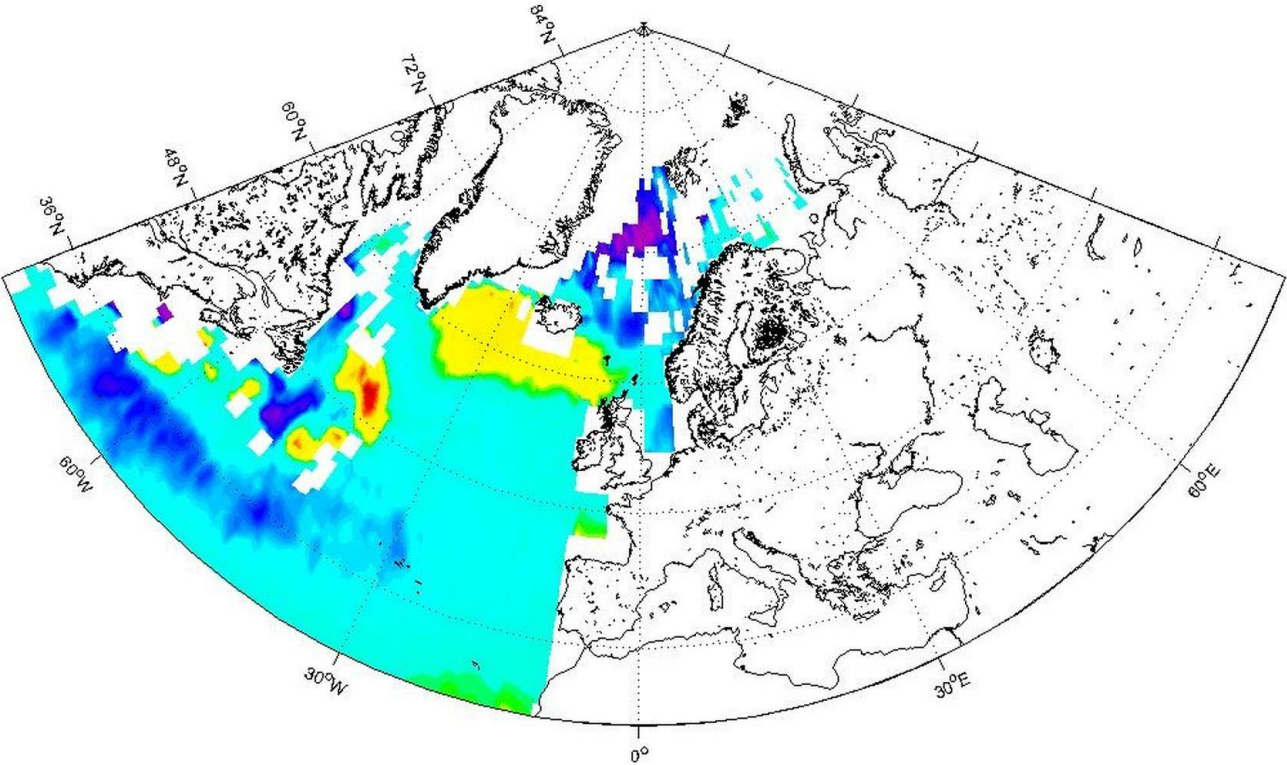
Table 1. Annual air-sea CO₂ fluxes (in Pg) using different k parameterizations. The values in parentheses are fluxes normalized to Nightingale et al., 2000 (as in Fig. 6)

	Global	Arctic	North Atlantic	Southern Ocean
Nightingale et al., 2000	-1.30 (1.00)	-0.102 (1.00)	-0.382 (1.00)	-0.72 (1.00)
Ho et al., 2006	-1.42 (1.09)	-0.106 (1.04)	-0.402 (1.05)	-0.76 (1.06)
Wanninkhof and McGillis, 1999	-1.73 (1.33)	-1.130 (1.28)	-0.490 (1.29)	-0.93 (1.30)
Wanninkhof, 2014	-1.40 (1.08)	-0.105 (1.03)	-0.398 (1.04)	-0.76 (1.05)
McGillis et al., 2001	-2.15 (1.65)	-0.147 (1.44)	-0.557 (1.46)	-1.08 (1.49)
OceanFlux GHG wind driven	-1.98 (1.52)	-0.138 (1.36)	-0.560 (1.47)	-1.14 (1.58)
OceanFluxGHG backscatter	-1.88 (1.44)	-0.130 (1.27)	-0.526 (1.38)	-1.09 (1.51)

661
662 a)

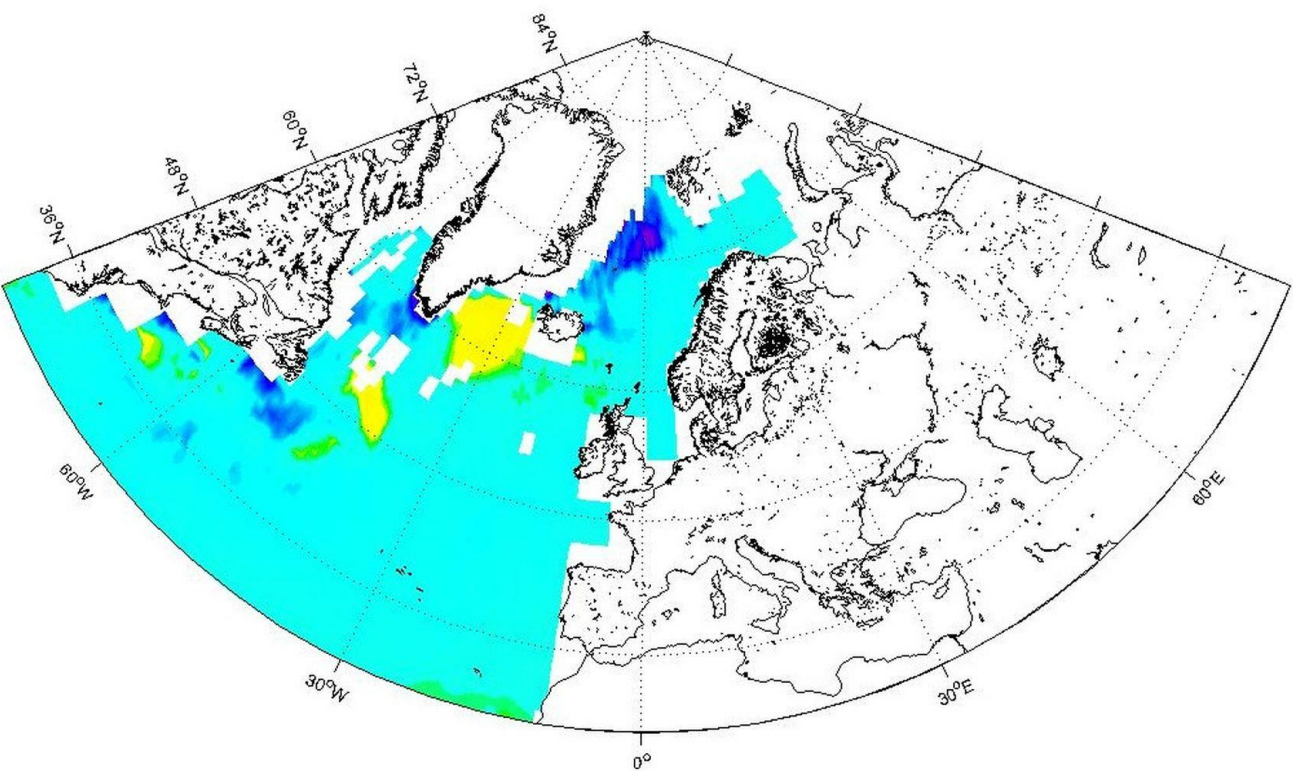


663
664 b)

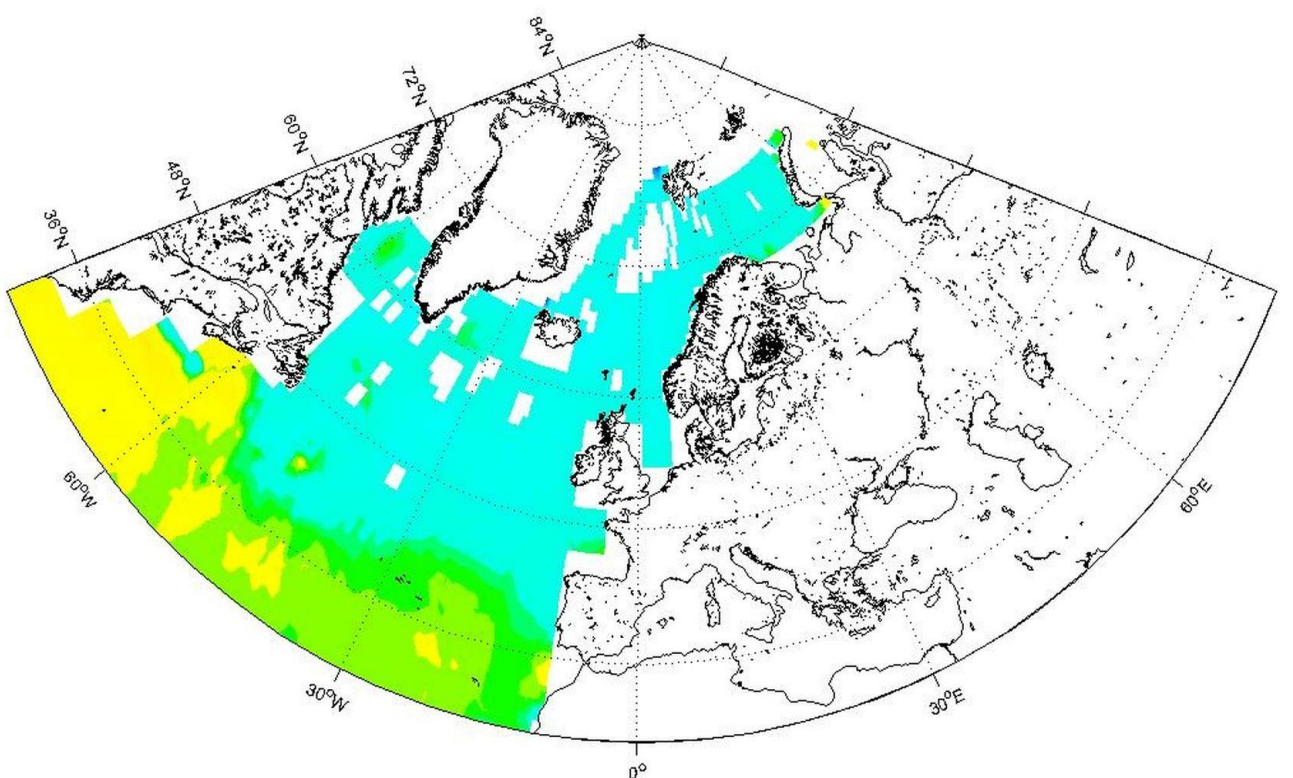


665
666 (mg C m⁻² day⁻¹)

667
668 c)

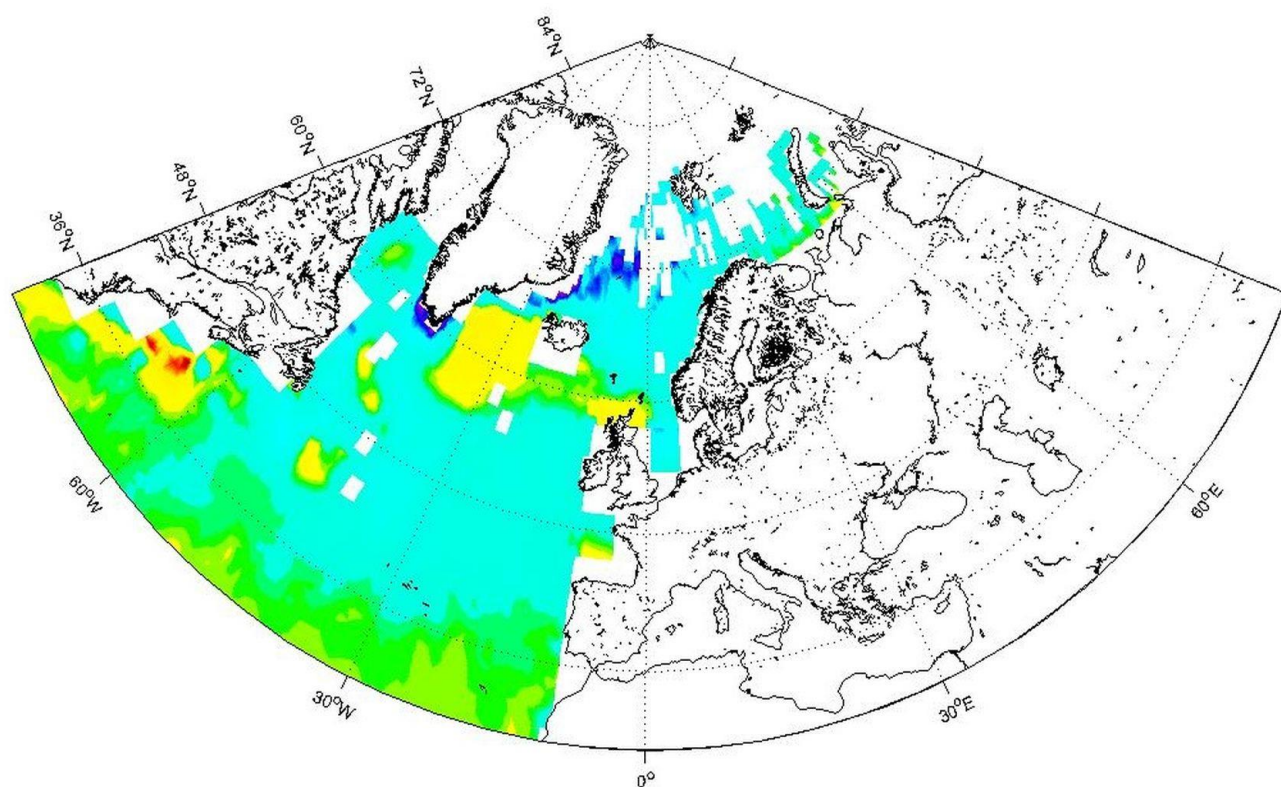


669
670 d)



671
672
673 (mg C m⁻² day⁻¹)

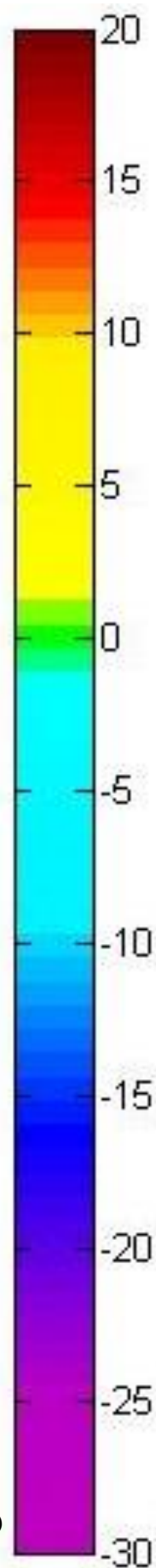
674
675 e)



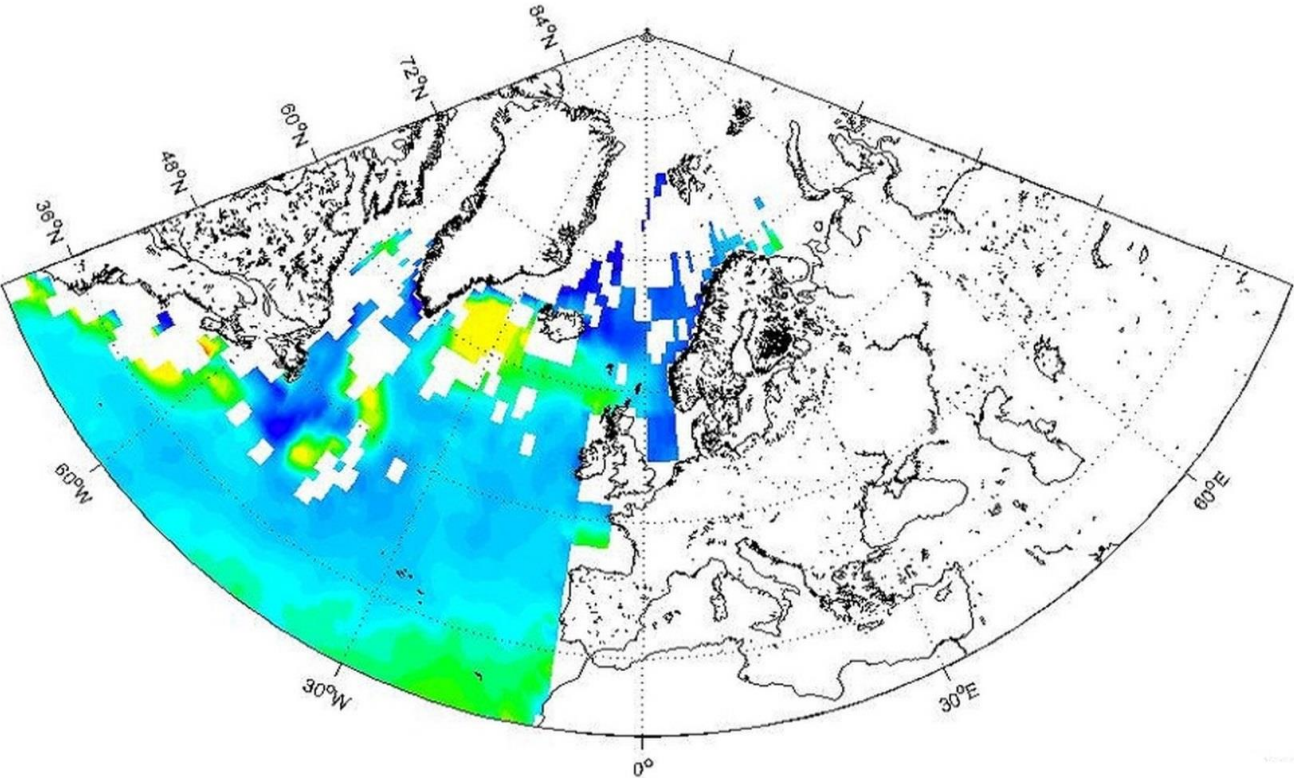
676
677 Figure 1. Seasonal and annual mean air-sea fluxes of CO₂ (mg C m⁻² day⁻¹) in the North Atlantic,
678 using Nightingale et al. (2000) *k* parameterization and the Takahashi et al. (2009) climatology a)
679 annual, b) DJF (winter), c) MAM (spring), d) JJA (summer), e) SON (autumn). The gaps (white
680 areas) are due to missing data, land and ice masks.

681
682
683
684
685
686
687
688
689
690
691
692
693
694
695
696
697
698
699

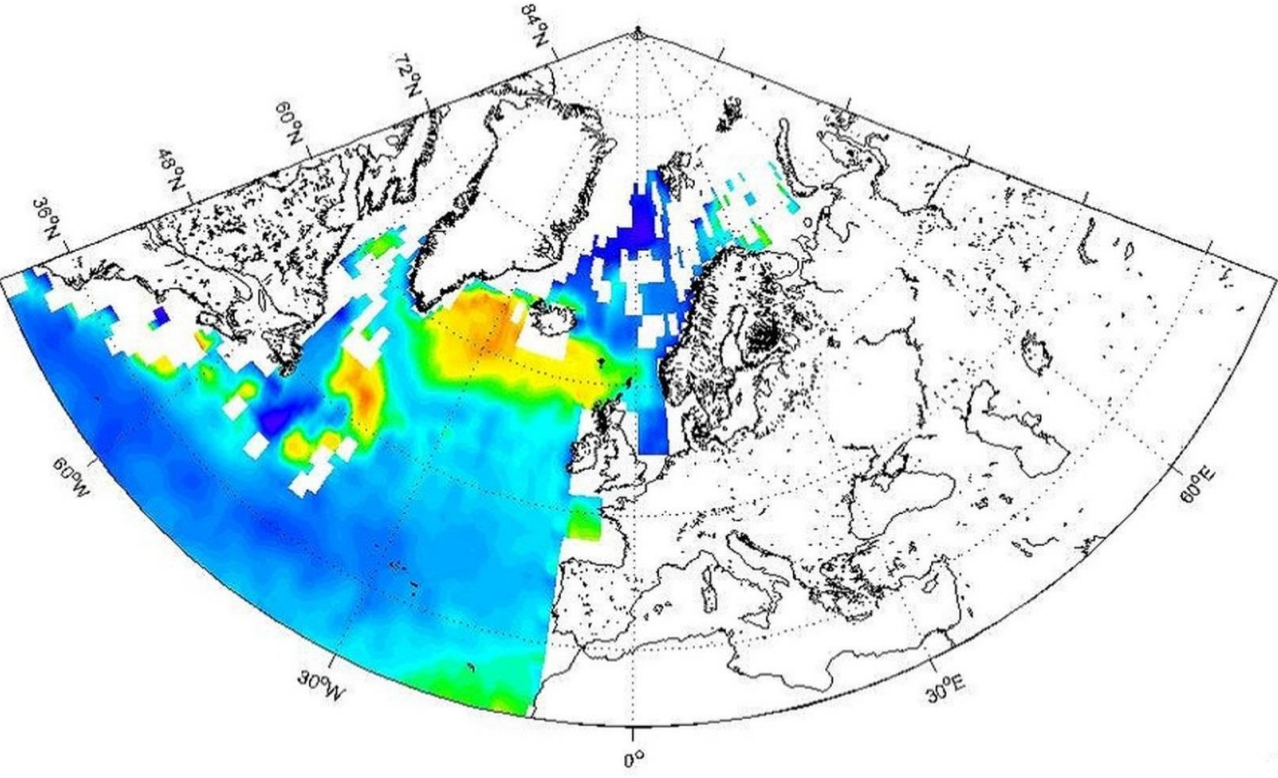
(mg C m⁻² day⁻¹)



700
701 a)

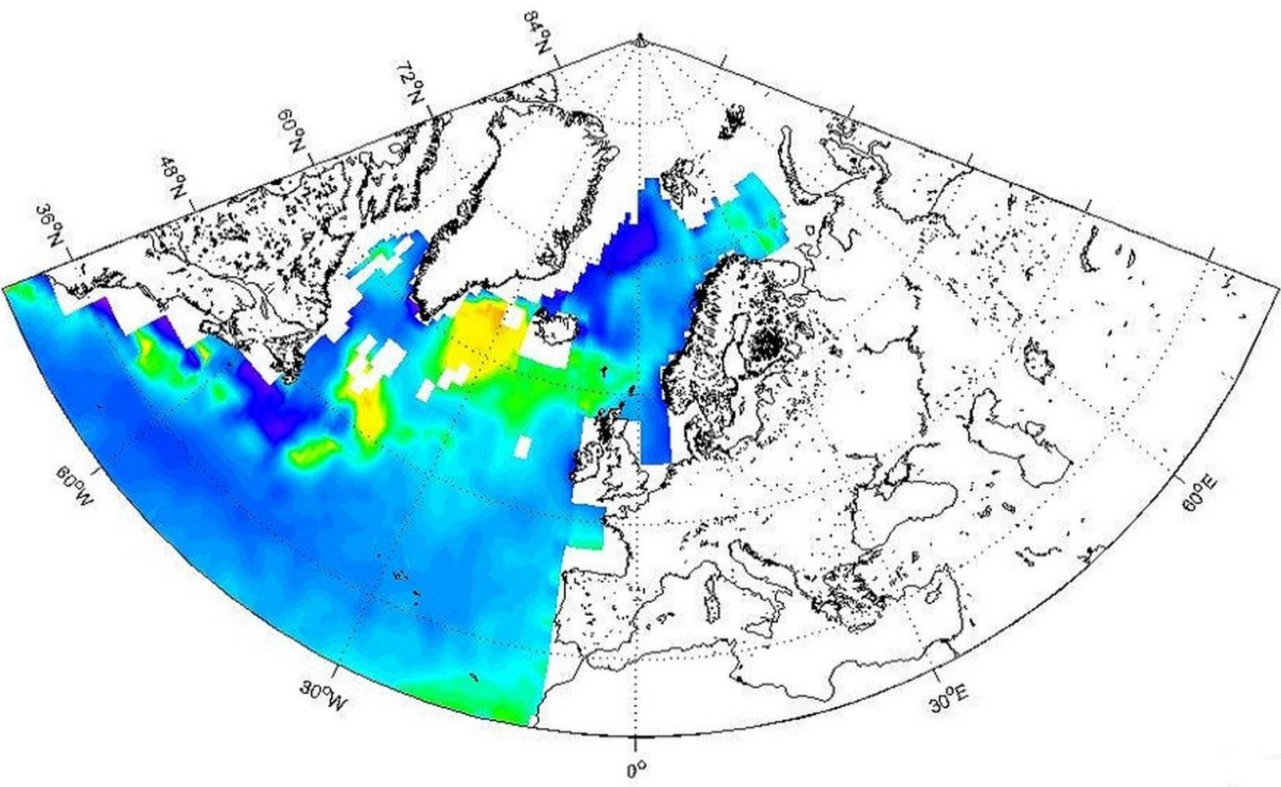


702
703 b)

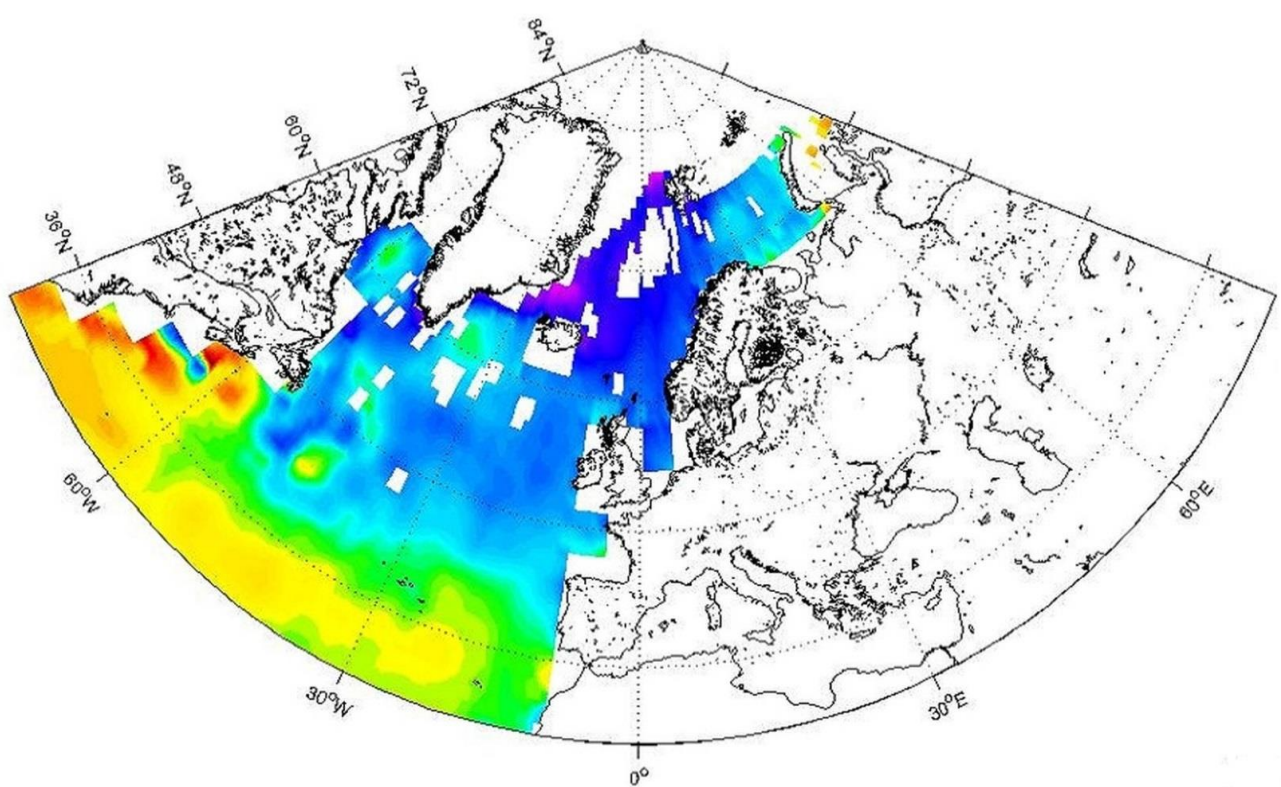


704
705 (μatm)

706
707 c)

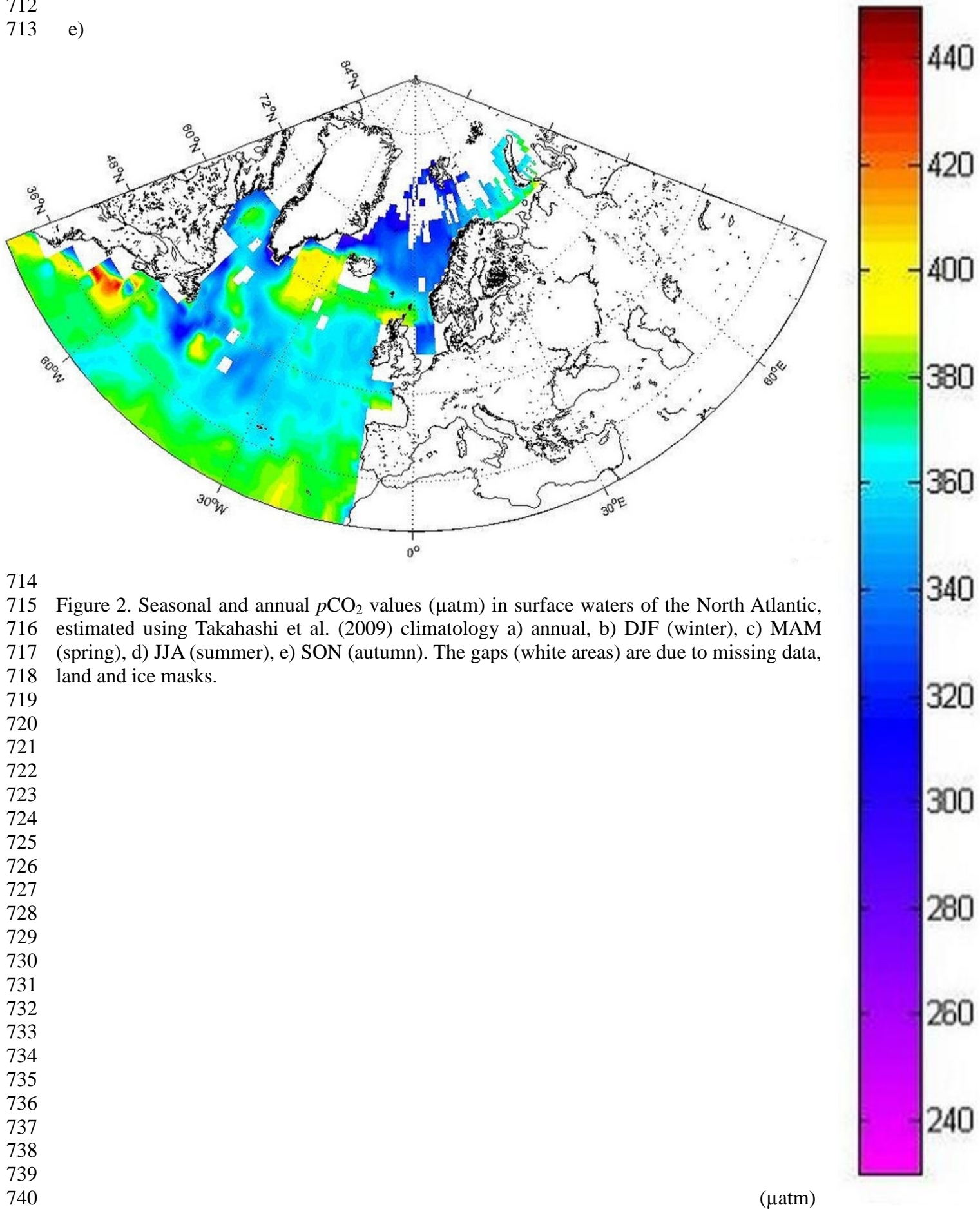


708
709 d)

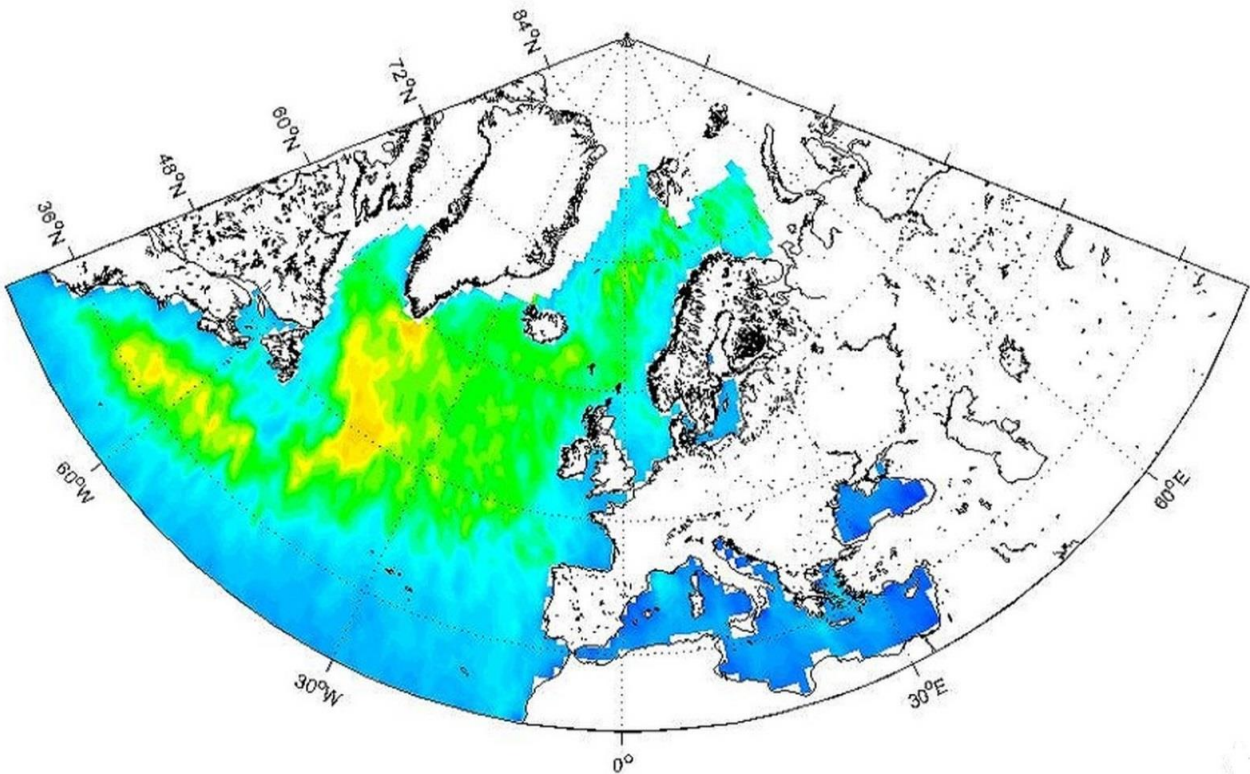


710
711 (μatm)

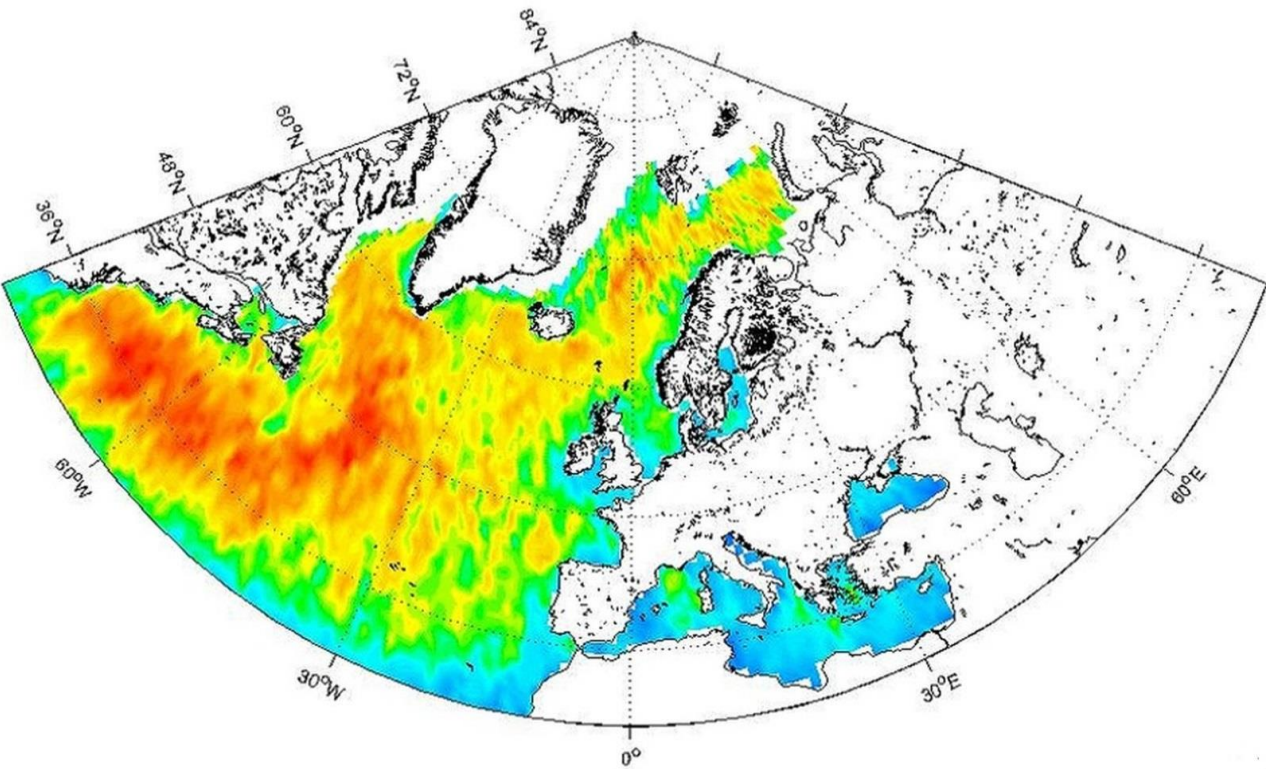
712
713 e)



741
742 a)

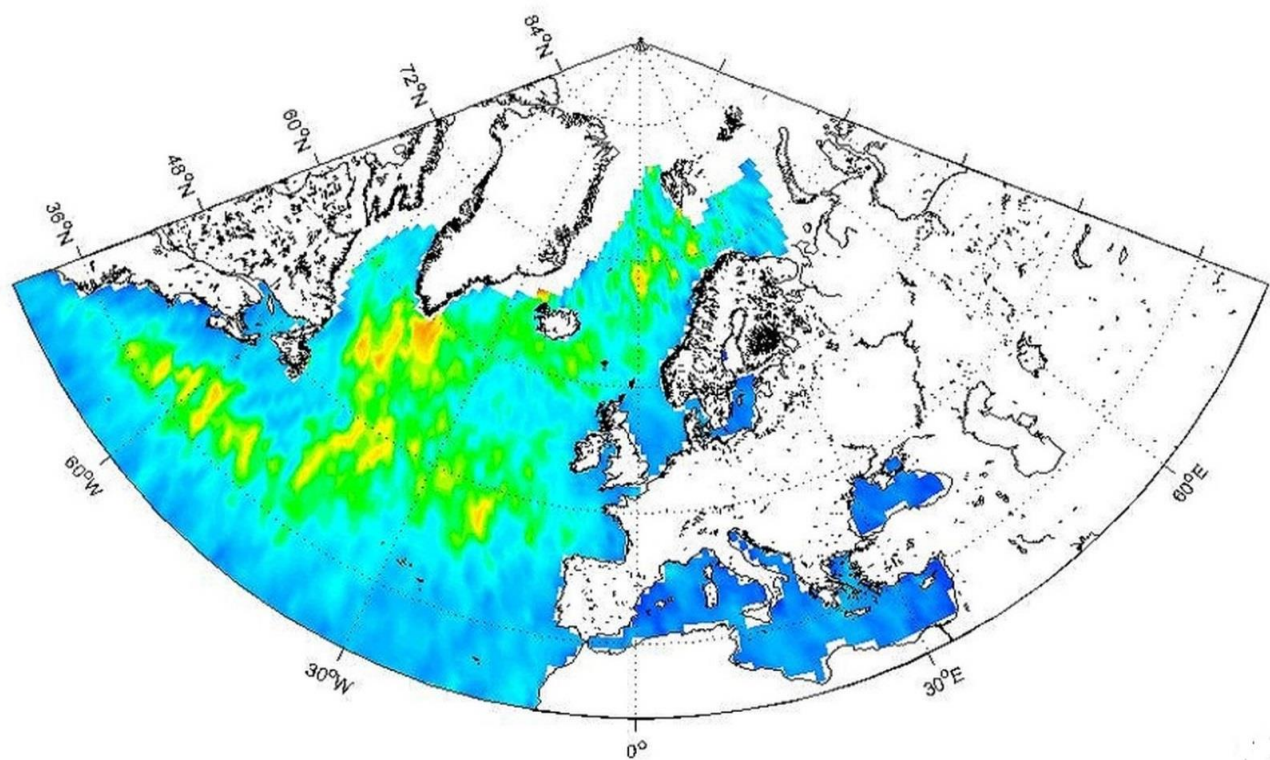


743
744 b)

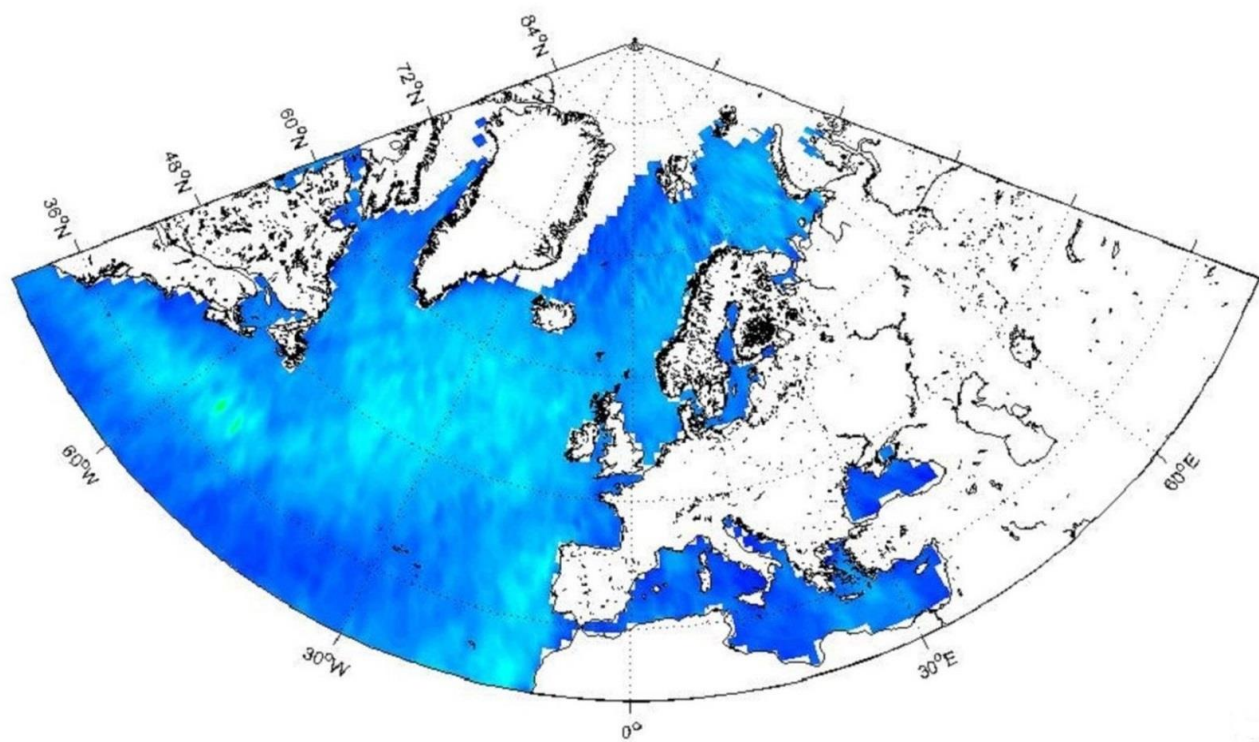


745 (ms^{-1})

746
747 c)

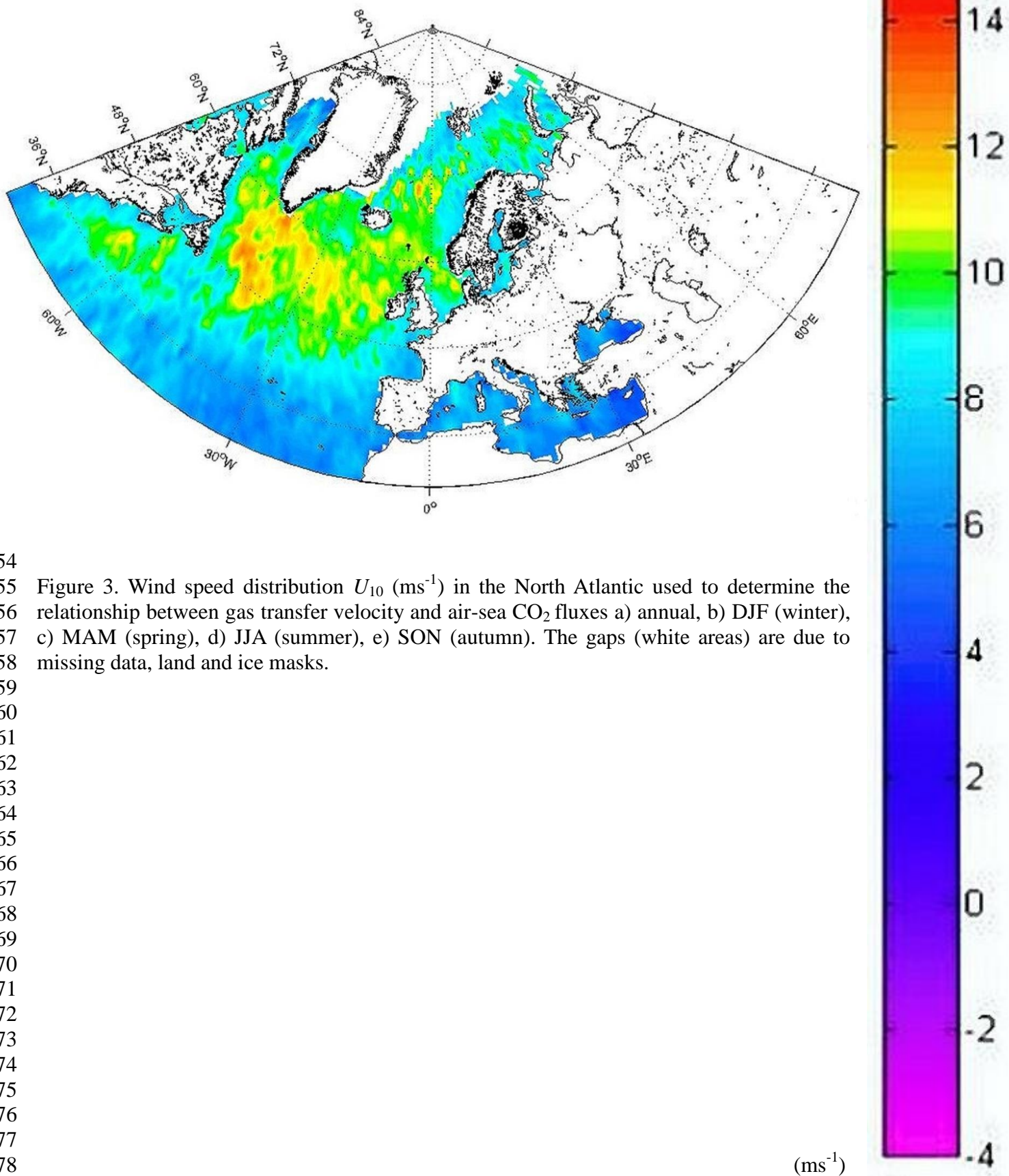


748
749
750 d)



751 (ms⁻¹)

752
753 e)

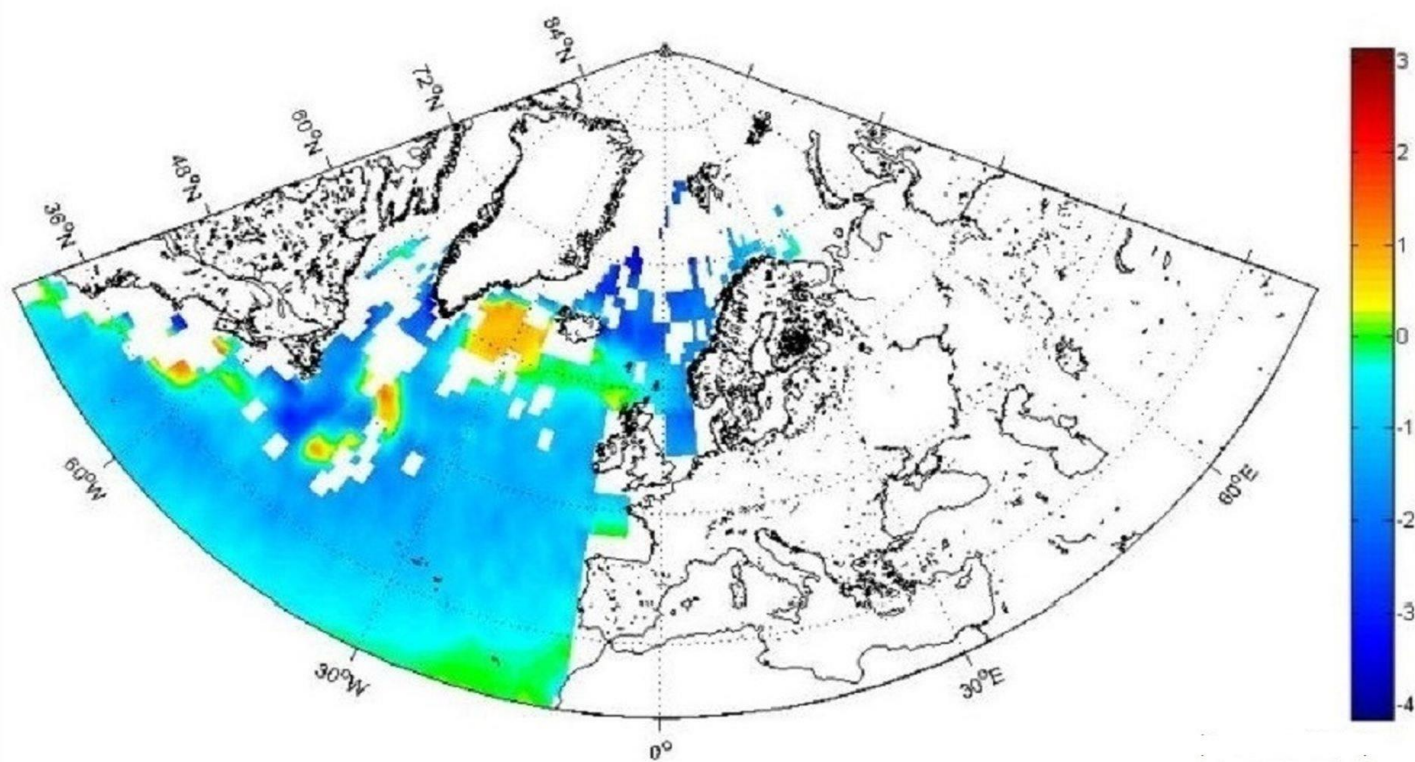


754
755 Figure 3. Wind speed distribution U_{10} (ms^{-1}) in the North Atlantic used to determine the
756 relationship between gas transfer velocity and air-sea CO_2 fluxes a) annual, b) DJF (winter),
757 c) MAM (spring), d) JJA (summer), e) SON (autumn). The gaps (white areas) are due to
758 missing data, land and ice masks.

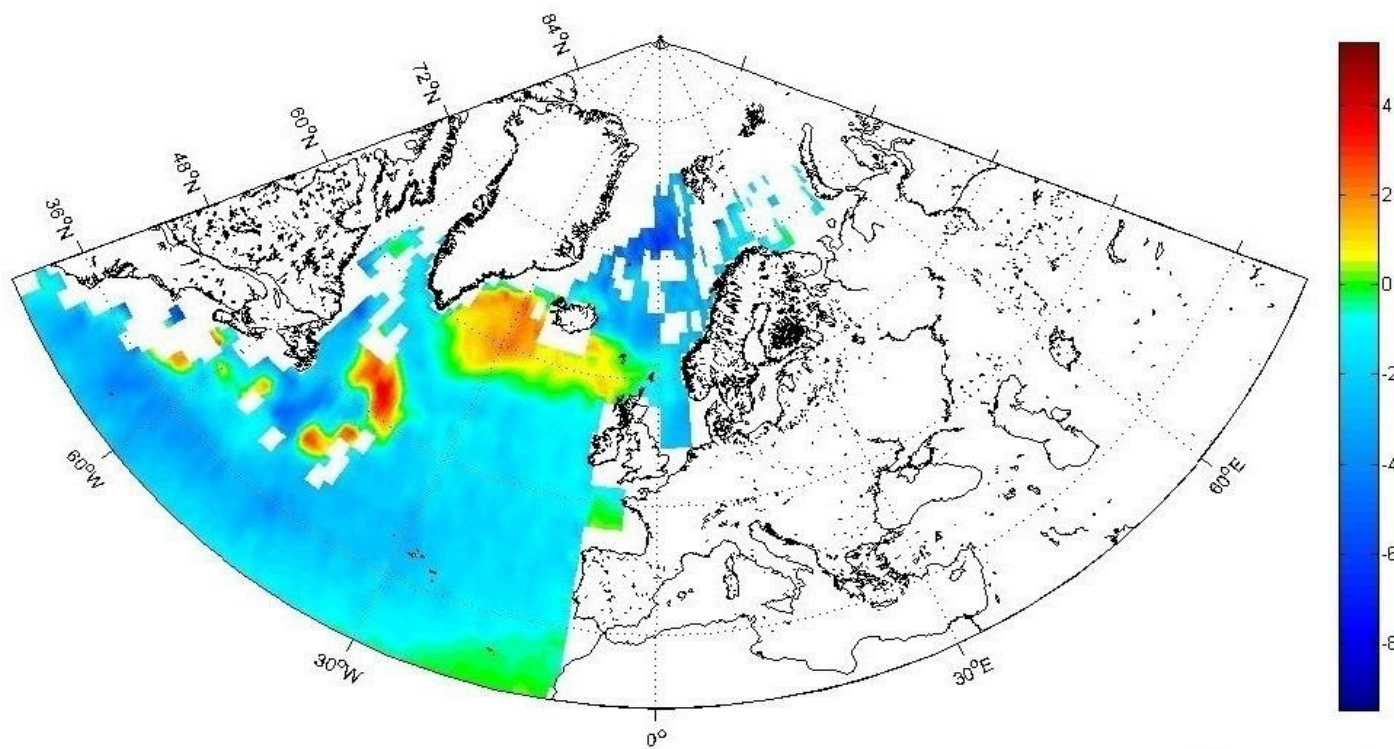
759
760
761
762
763
764
765
766
767
768
769
770
771
772
773
774
775
776
777
778

(ms^{-1})

779
780 a)

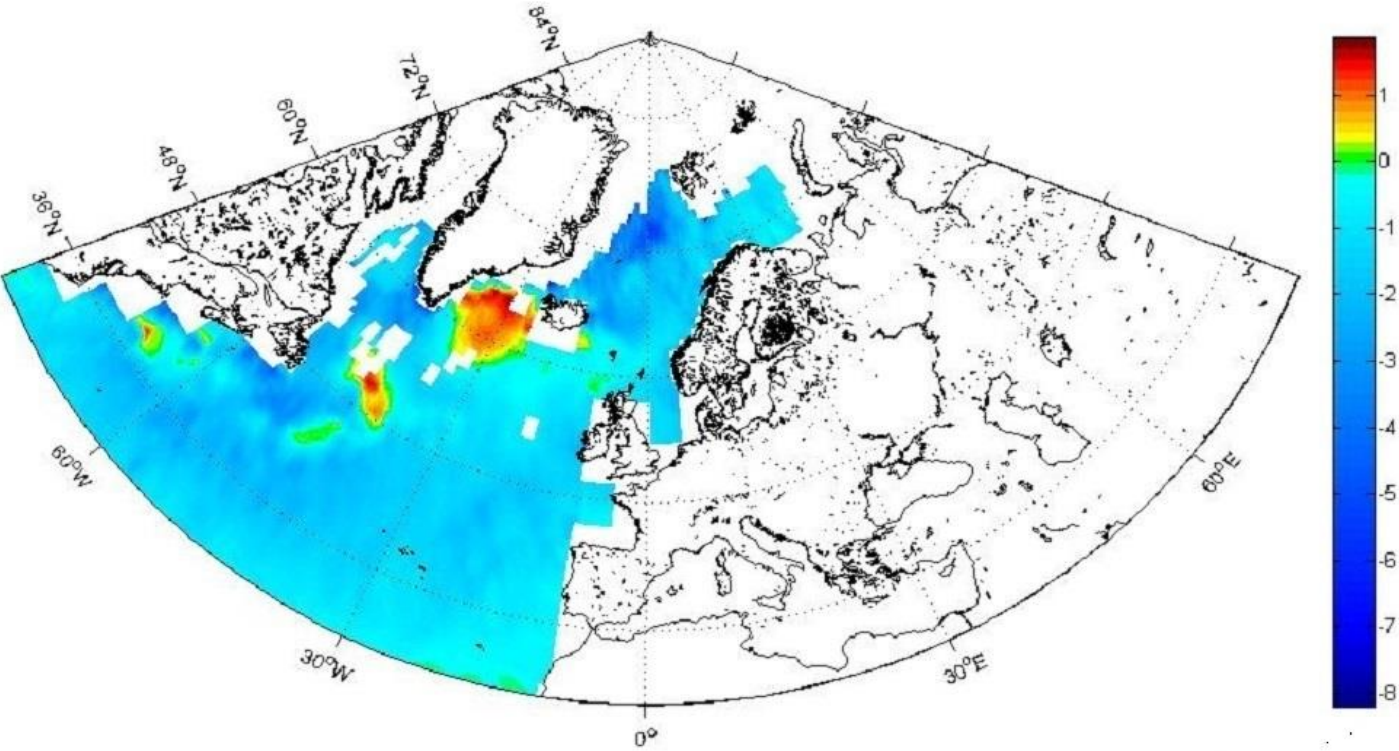


781 (mg C m⁻² day⁻¹)
782 b)

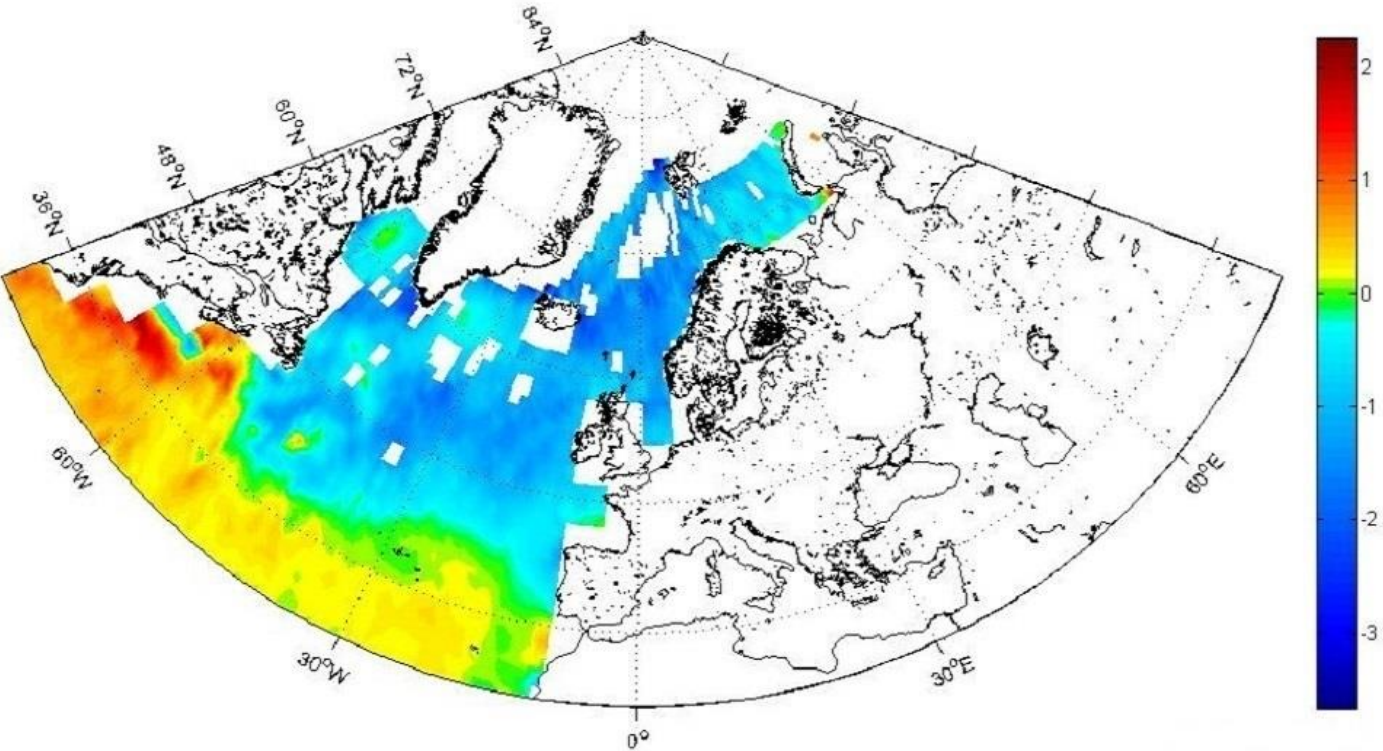


783 (mg C m⁻² day⁻¹)
784
785

786
787 c)

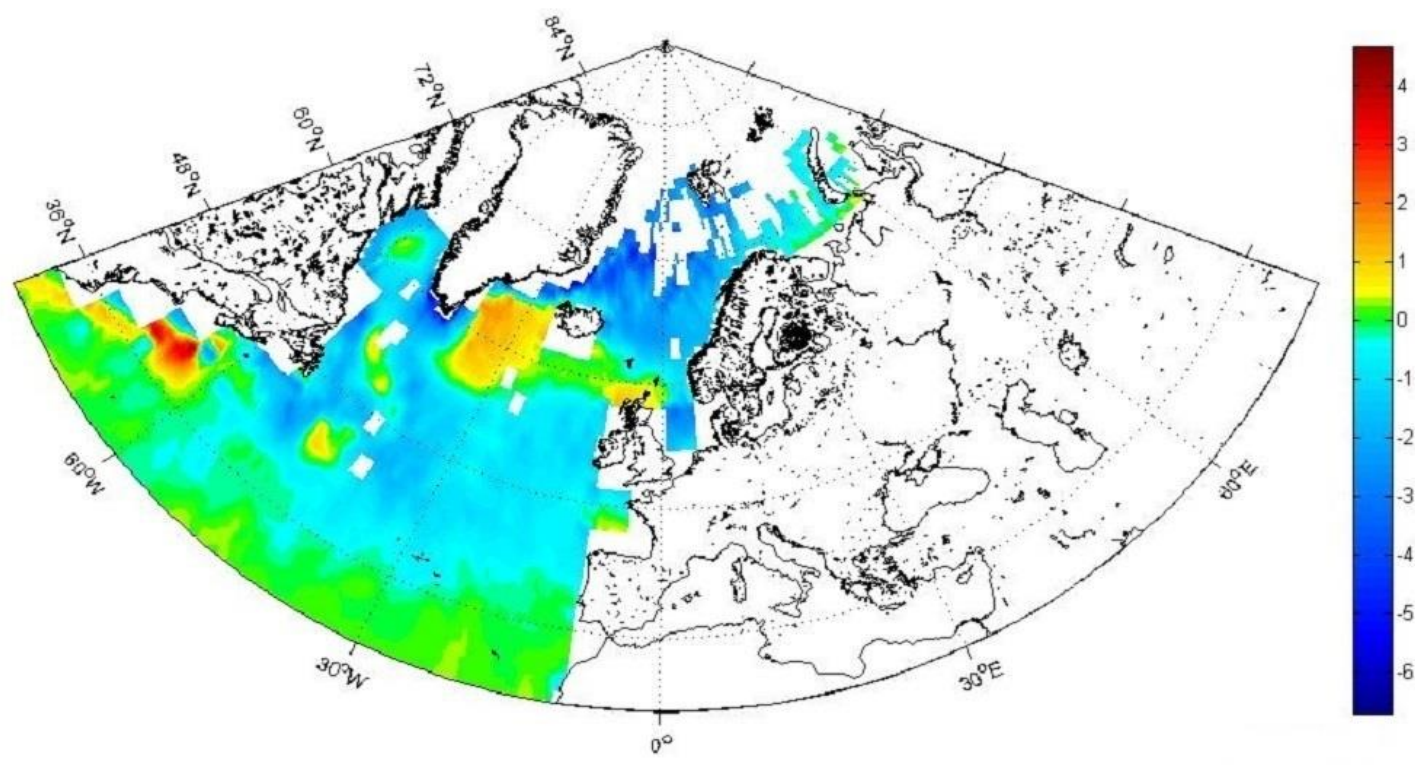


788 (mg C m⁻² day⁻¹)
789 d)



790 (mg C m⁻² day⁻¹)
791
792

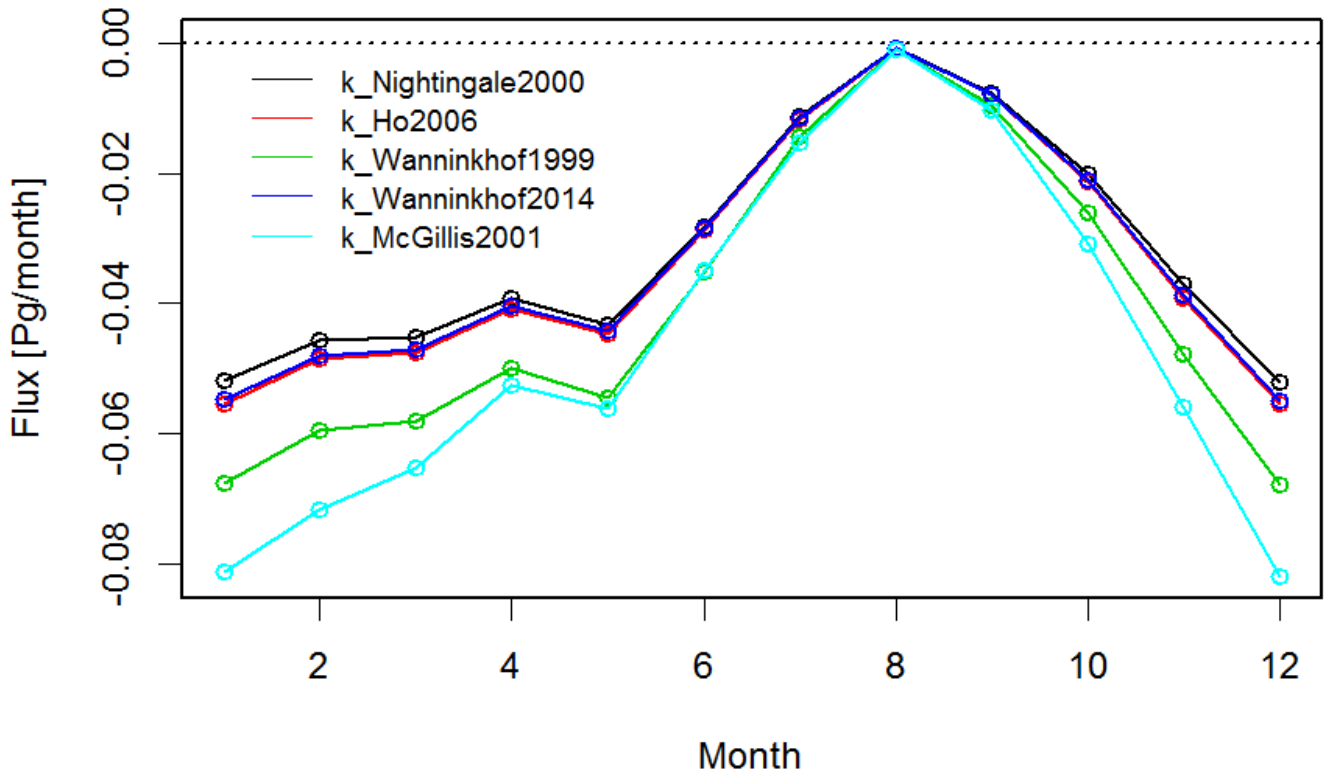
793
794 e)



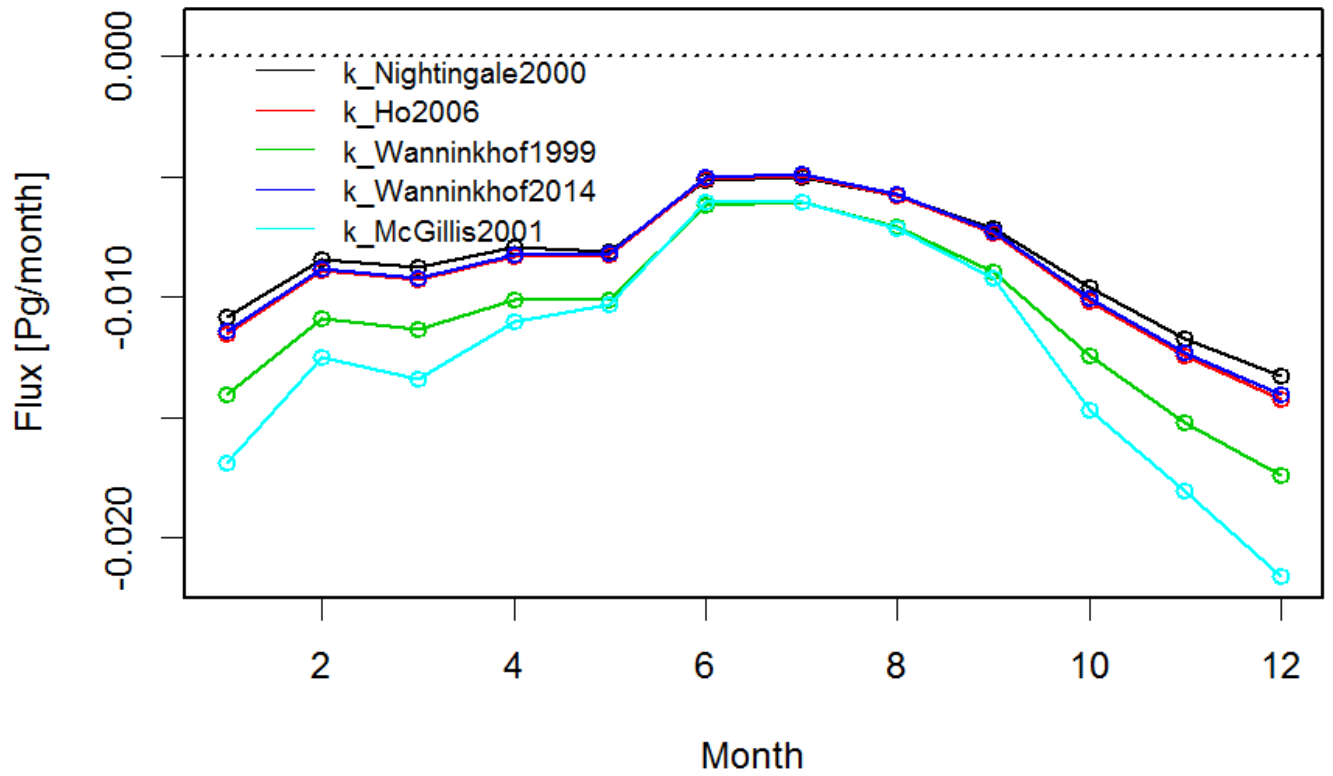
795 (mg C m⁻² day⁻¹)
796

797 Figure 4. Differences maps for the air-sea CO₂ fluxes (mg C m⁻² day⁻¹) in the North Atlantic, between
798 a cubed and a squared parameterization (Wanninkhof and McGillis 1999 and Wanninkhof 2014) a)
799 annual, b) DJF (winter), c) MAM (spring), d) JJA (summer), e) SON (autumn). The gaps (white
800 areas) are due to missing data, land and ice masks.

801
802 a)

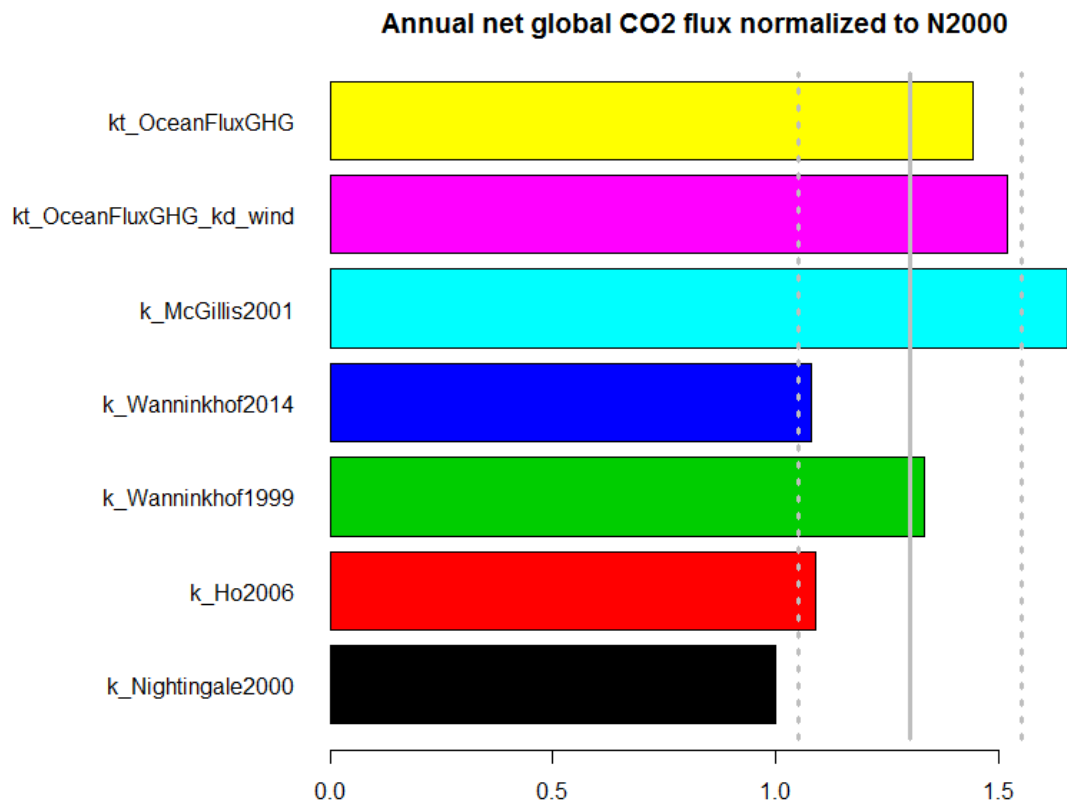


803
804 b)

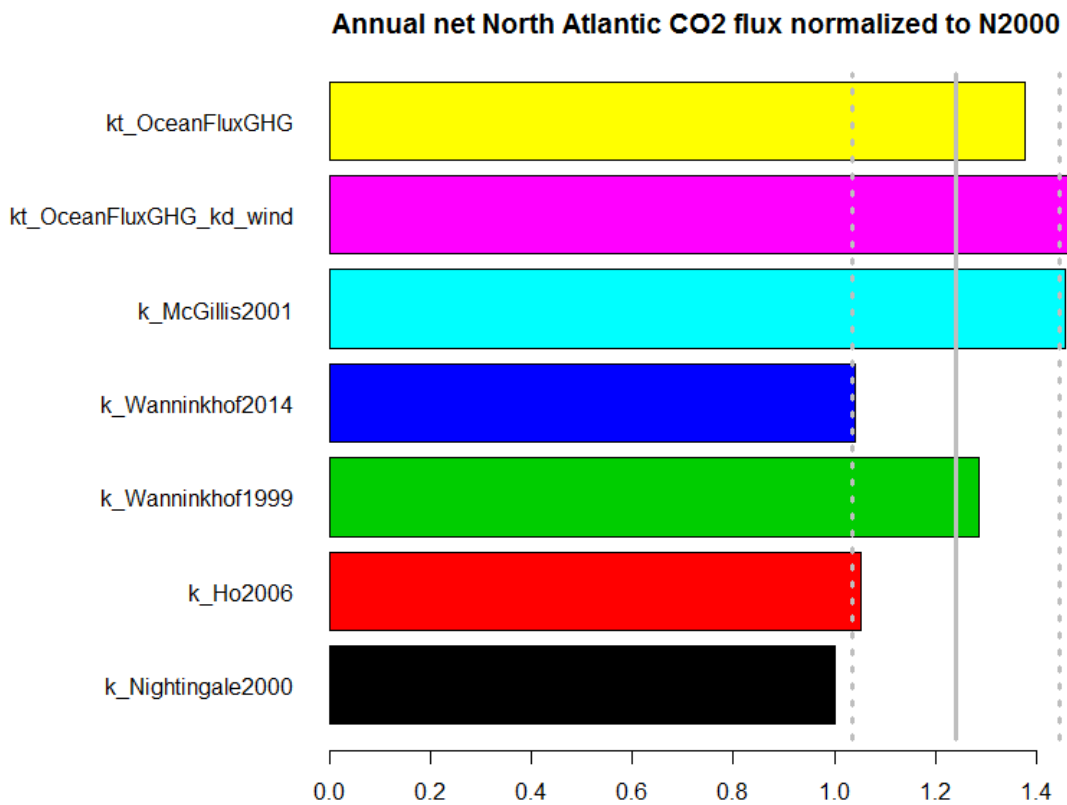


805
806 Figure 5. Monthly values of CO₂ air-sea fluxes (Pg/month) for the five parameterizations (eq. 4-8)
807 a) the North Atlantic, b) the European Arctic.
808

809
810 a)

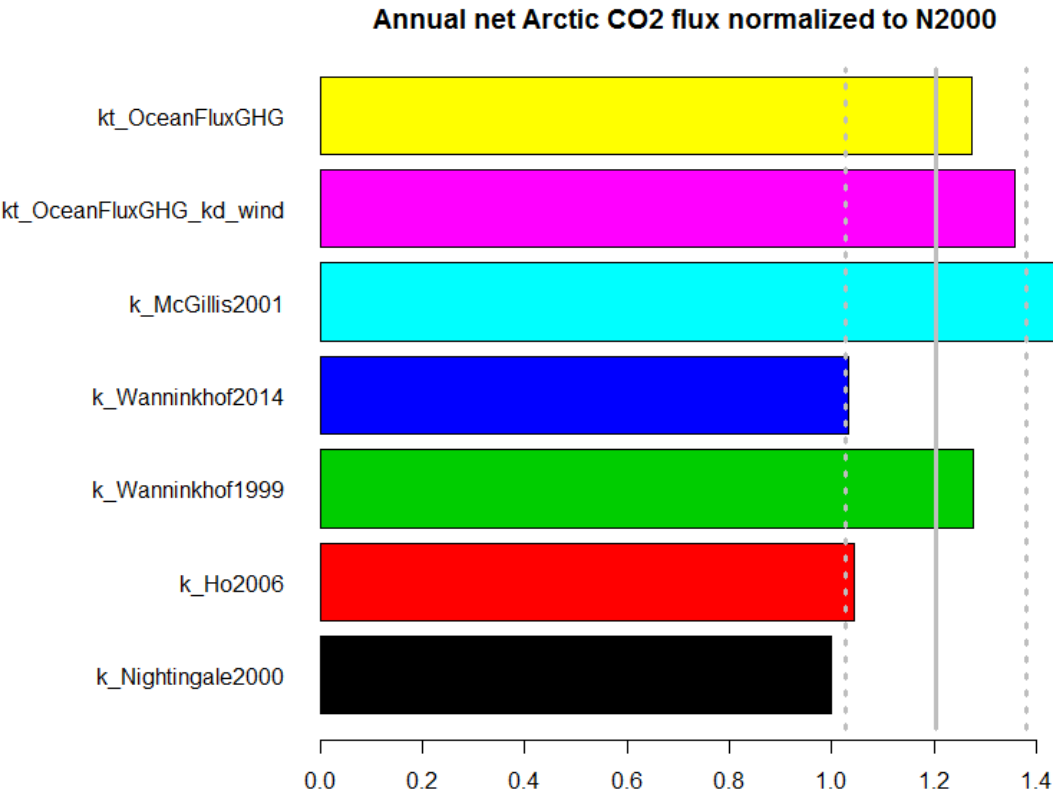


811
812
813 b)

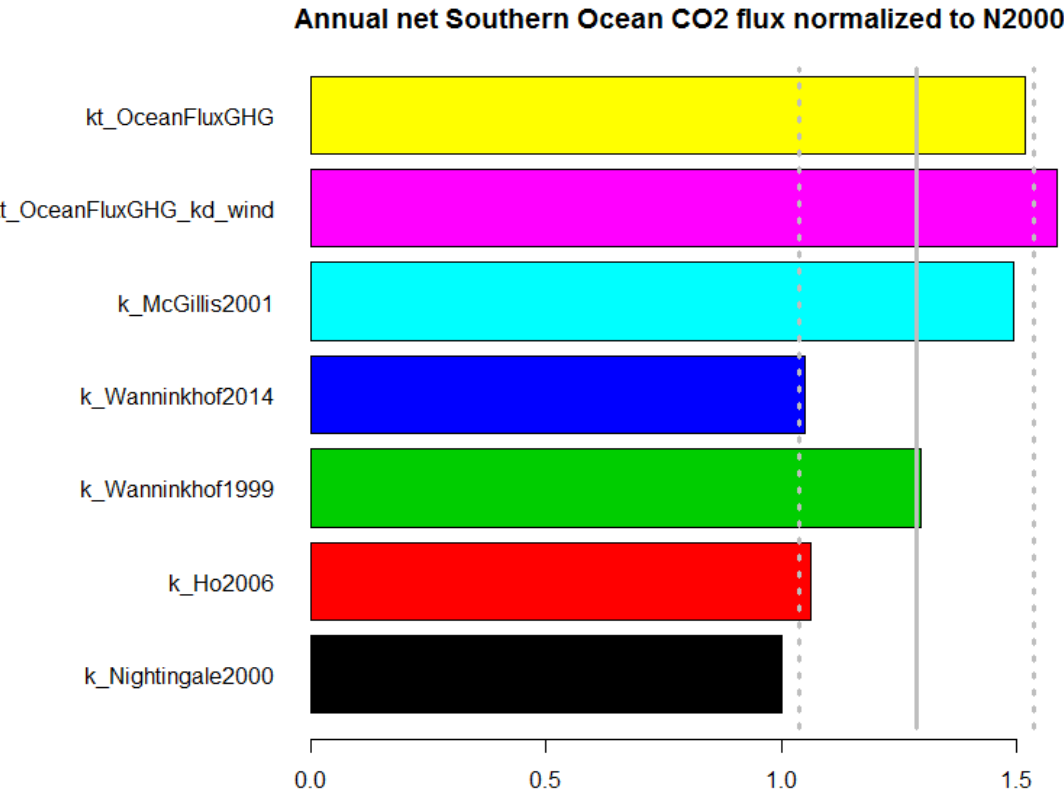


814
815
816
817
29

818 c)

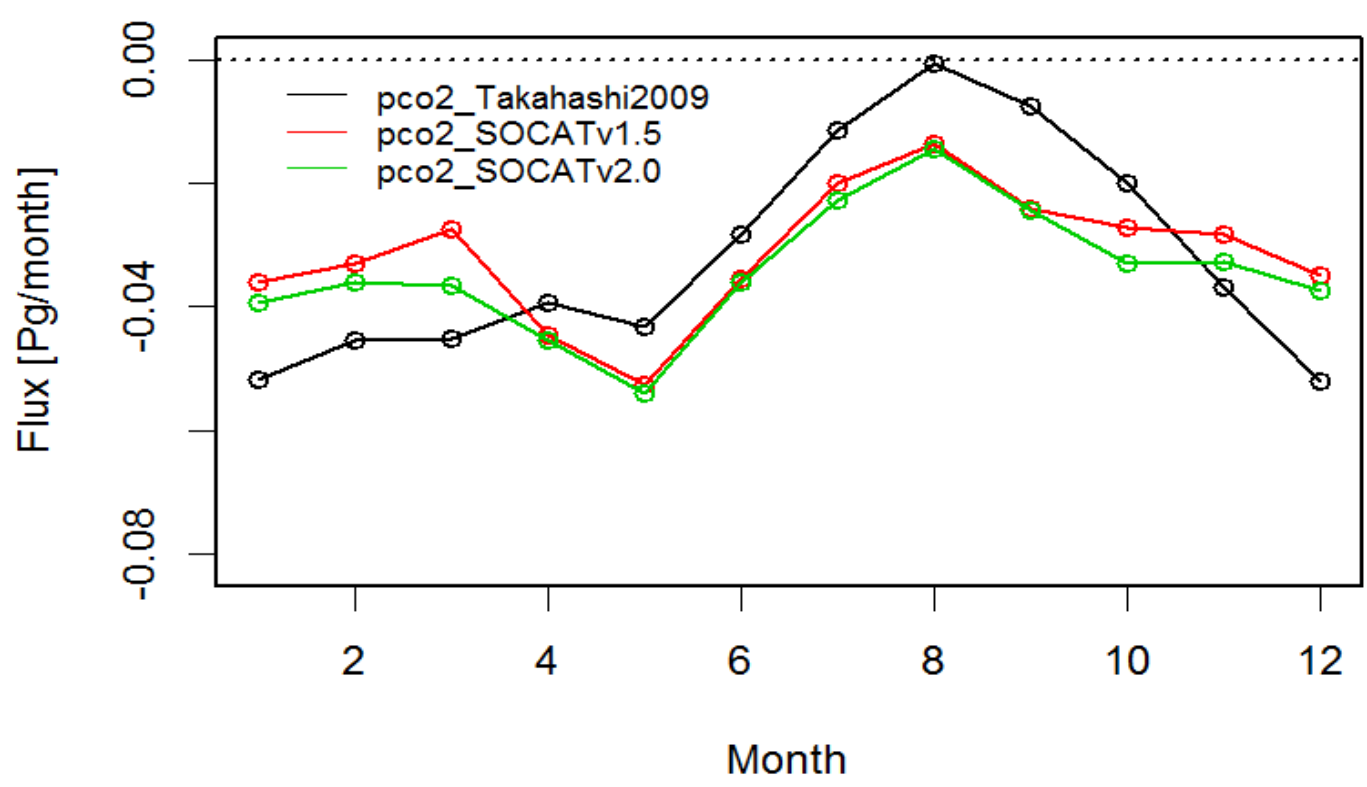


819
820 d)

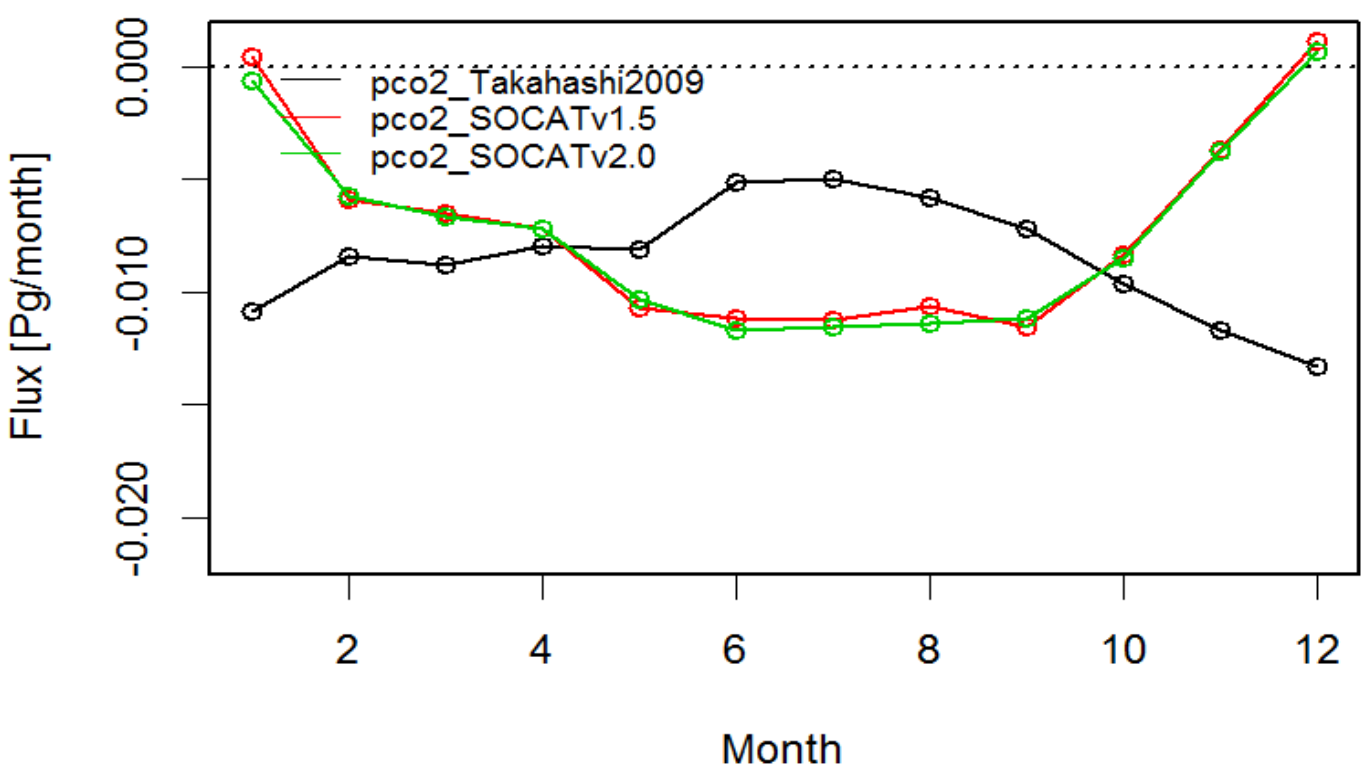


821
822 Figure 6. Annual air-sea fluxes of CO₂ for the five (eq. 4-8) parameterizations as well as for
823 backscatter (default) and wind driven OceanFluxGHG parameterizations normalized to flux values
824 of Nightingale et al. (2000) *k* parameterization (see text) a) globally, b) the North Atlantic, c) the
825 European Arctic, d) the Southern Ocean. Average values for all parameterization and standard
826 deviations are marked as vertical gray lines.

827
828 a)

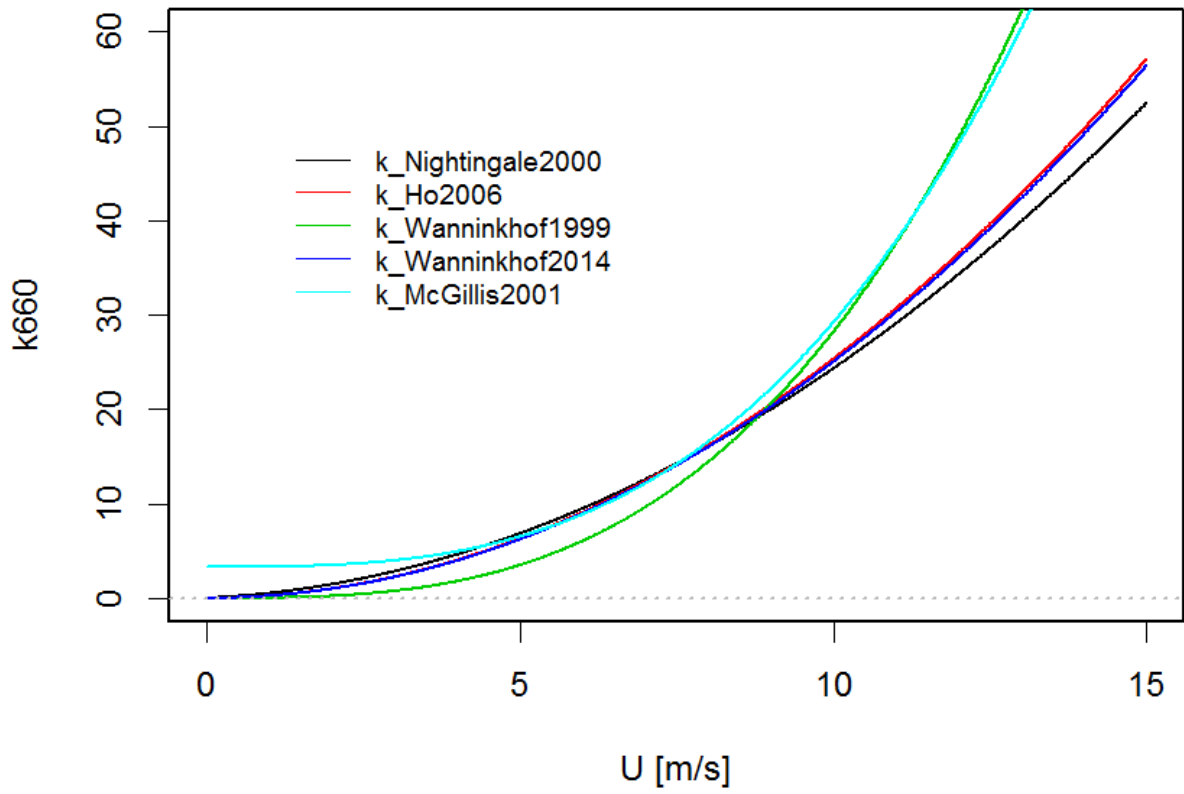


829
830 b)



831
832 Figure 7. Comparison of monthly air-sea CO₂ fluxes calculated with different *p*CO₂ datasets
833 (Takahashi et al., 2009, SOCAT v. 1.5 and 2.0) using the same *k* parameterization (Nightingale et
834 al., 2000) a) the North Atlantic, b) the European Arctic.

835
836



837
838 Figure 8. Different k_{660} parameterizations as a function of wind speed.